COMPLEX DISTILLATION CALCULATIONS

ABSTRACT

Unit operations such as flash and distillation processes are common in the chemical and petroleum industries. Some common computational problems encountered while simulating these operations include difficulty in predicting the phase behavior of mixtures at high pressures and the extreme sensitivity of the calculations (and, perhaps, of operations themselves) to process variables. In the past these calculations were carried out in the real domain. A radically different approach to simulating flash and distillation operations has been proposed recently and further explored in the present thesis. Examples showing the features of complex domain calculations are also presented. It is concluded that complex calculations can help in obtaining real solutions to process engineering problems and may give good insight into the nature of the problem when real calculations fail.

ACKNOWLEDGEMENT

I am grateful to Dr. Ross Taylor for his valuable guidance and inspiration throughout the course of this work. I hereby also thank Dr. Angelo Lucia for his suggestions and constant support at times of difficulty. My acknowledgements are due to the Department of Chemical Engineering, Clarkson University, for having provided me with a Teaching Assistantship during the tenure of my study. I also appreciate the help given by Harry Kooijman, Xin-Zhou Guo and Jinxian Xu at different stages of my research. Finally, I convey my special note of appreciation to my parents and family who though far away have been constant sources of encouragement and because of whom the present work was possible.

CONTENTS

LIST OF FIGURES

LIST OF TABLES

1 INTRODUCTION

1.1 Background

Distillation has been employed for decades as the primary method of separation in chemical and petrochemical industries. The preeminence of distillation over other unit operations is unlikely to be displaced for many more years to come. Flash calculations are used to determine the phase condition of mixtures that need to be distilled.

Flash and distillation operations usually are simulated with the "equilibrium stage model". The vapor and liquid leaving an equilibrium stage are assumed to be in complete equilibrium with each other and the thermodynamic relations are used to relate the properties of the exiting streams. This equilibrium stage model was first used by Sorel (1893) to describe the rectification of alcohol. Since then this model has seen extensive use in the chemical and petroleum industries. A more detailed description of the model follows in Chapter 2.

Accurate prediction of thermodynamic properties is an important issue in the design and analysis of separation processes. The two methods used most often to predict the thermodynamic properties of a mixture are (i) the single model approach, where a single equation of state is used to represent both liquid and vapor properties and (ii) the mixed model approach wherein different models are used for liquid and vapor phases. The single model approach is

preferred especially in gas processing plants operating at high pressures close to the critical region where equilibrium properties change rapidly with pressure (Veerana and Rihani, 1984). Cubic equations of state (e.g. Soave-Redlich-Kwong and Peng-Robinson) are among the most popular methods used for estimating the equilibrium ratios of hydrocarbon mixtures at high pressure. However, the equation of state approach leads to certain computational difficulties in iterative phase equilibrium calculations such as trivial solutions or false convergences (Veerana et al., 1987). These difficulties arise in conditions in which only a single real root of the cubic compressibility polynomial exists for each phase. The calculation of a computed root that is "vapor-like" when a "liquid-like" root is needed can generate serious difficulties in the calculation of appropriate fugacities and K-values for the two phases. Though these difficulties have been encountered frequently in the past (see, for example, Gosset et al., 1986; Lawal, 1987), a radically different approach leading to a possible solution has not been presented until the work of Lucia and Taylor (1992).

Recently, Lucia et al. (1990) have shown that iterative maps (for example, direct substitution or Newton's method) can exhibit periodic or chaotic behavior when used to solve simple process model equations such as an equation of state. In their work, many examples from process engineering were shown to exhibit period doubling, aperiodicity and fractal basin boundaries. The examples they studied included flash and dew point

calculations of heterogeneous mixtures and finding roots to the SRK equation of state. Lucia and Taylor (1992) have shown that the iterative use of complex roots to cubic equations of state within equilibrium flash calculations may offer advantages in convergence especially in situations where only one real root exists.

1.2 Objectives

The goal of the present work has been to extend the work of Lucia and Taylor and to carry out different flash and distillation calculations in the complex domain using an equilibrium stage model. We wish to determine if complex solutions exist to the distillation model equations and to see if there are any computational benefits to carrying out distillation calculations in the complex domain.

Chapter 2 describes the primary equations employed to model flash and distillation operations and also the method used to solve these equations. A few examples portraying the significance and some of the advantages of carrying out complex calculations are presented in Chapter 3.

2 FLASH AND DISTILLATION CALCULATIONS

Equilibrium stage models of flash and distillation operations are presented in the following sections. The numerical methods that are employed to solve the primary equations are also discussed. In addition, a complete description of the procedure adopted to generate the initial values of all unknown variables is provided.

2.1 MATHEMATICAL MODELS

2.1.1 Flash Equations

Flash calculations are the single most important chemical process calculations. They are used to determine the phase conditions of fluids. Isothermal flash modules constitutes one of the most frequently performed calculations in modularly structured process simulators and much has been done in the development of reliable and fast converging algorithms.

A schematic diagram of a single stage flash is shown in Figure 2.1. The equations used to model the flash operation include:

a) Total Mass Balance

$$M \equiv V + L - F = 0 \tag{1}$$

b) Component Mass Balances

$$M_i \equiv Vy_i + Lx_i - Fz_i = 0 \tag{2}$$

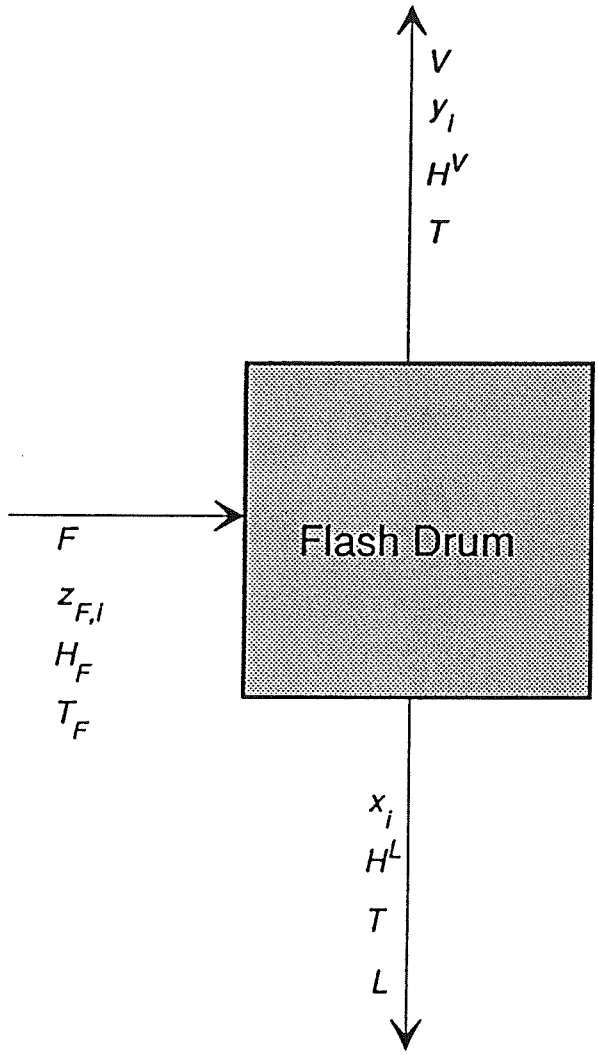

Figure 2.1 Schematic Diagram of a Flash drum

c) Equilibrium Relations

$$E_i \equiv K_i x_i - y_i \tag{3}$$

d) Summation Equations

$$S^L \equiv \sum_{i=1}^{c} x_i = 0 \tag{4}$$

$$S^V \equiv \sum_{i=1}^{c} y_i = 0 \tag{5}$$

e) Energy Balance Equation

$$H \equiv V H^V + L H^L - F H^F + Q = 0 \tag{6}$$

The material balance, equilibrium relations and a modified summation equation resulting from the combination of the two summation equations represented as

$$S^{V-L} \equiv \sum_{i=1}^{c} y_i - \sum_{i=1}^{c} x_i = 0 \tag{7}$$

number $2c+2$ independent equations. The $2c+2$ variables obtained by solving the above set of equations are the c liquid mole fractions, x_i, the c vapor mole fractions, y_i, and the liquid and vapor flow rates L and V. In QP flashes the temperature also is not known prior to solving the equations.

2.1.2 MESH Equations

The schematic diagram of an equilibrium stage in a column is shown in Figure 2.2. The acronym MESH stands for the model equations representing

the equilibrium stage and they are:

(a) Total Mass Balance

$$M_j^T \equiv (1+r_j^V)V_j + (1+r_j^L)L_j - V_{j+1} - L_{j-1} - F_j = 0 \qquad (8)$$

(b) Component Mass Balances

$$M_{ij} \equiv (1+r_j^V)V_j y_{ij} + (1+r_j^V)L_j x_{ij} - V_{j+1}y_{i,j+1} - L_{j-1}x_{i,j-1} - F_j z_{ij} = 0 \qquad (9)$$

where the r_j are the ratios of the sidestream flow to interstage flows

$$r_j^V = \frac{W_j}{V_j} \qquad r_j^L = \frac{U_j}{L_j} \qquad (10)$$

(c) Equilibrium Relations

$$E_{ij} \equiv K_{ij}x_{ij} - y_{ij} = 0 \qquad (11)$$

(d) Summation Equations

$$S_j^L \equiv \sum_{i=1}^{c} x_{ij} - 1 = 0 \qquad (12)$$

$$S_j^V \equiv \sum_{i=1}^{c} y_{ij} - 1 = 0 \qquad (13)$$

Combining the above two equations into a single independent equation, the summation equation becomes:

$$S_j^{V-L} \equiv \sum_{i=1}^{c} y_{ij} - \sum_{i=1}^{c} x_{ij} = 0 \qquad (14)$$

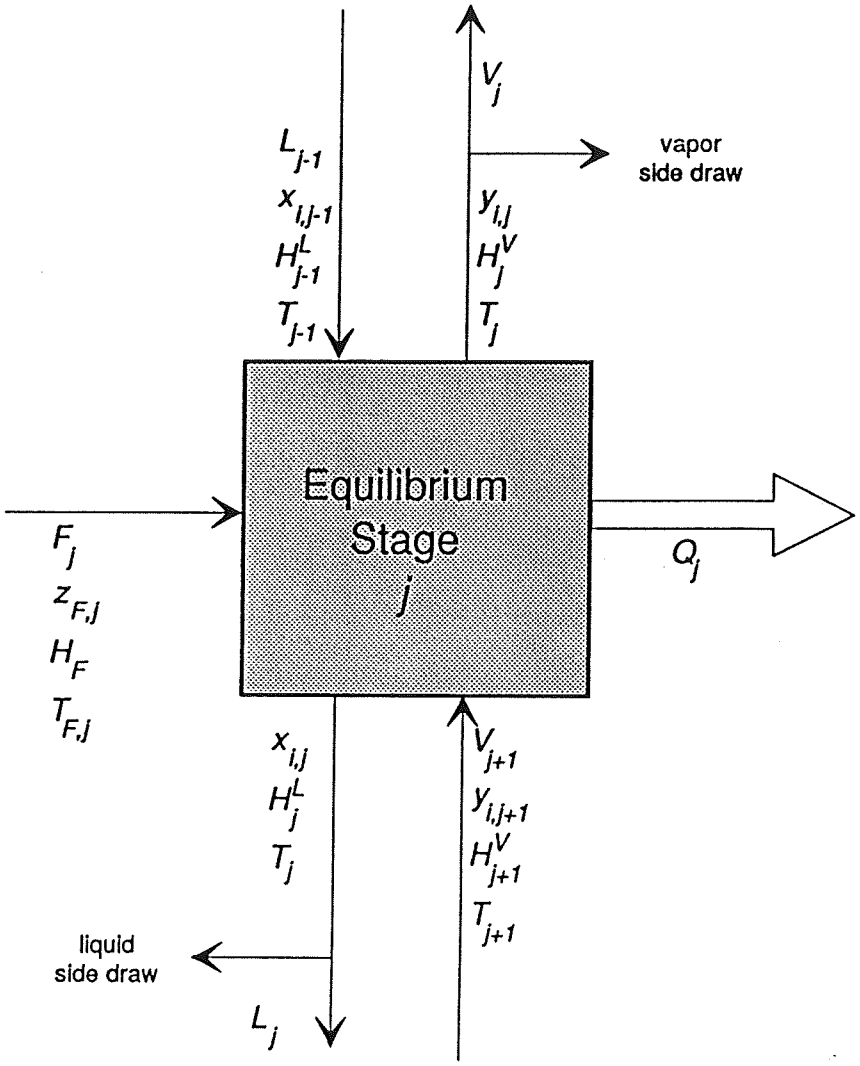

Figure 2.2 Schematic Diagram of an Equilibrium Stage

(e) Heat Balance Equations

$$H_j \equiv (1+r_j^V)\,V_j H_j^V + (1+r_j^L)\,L_j H_j^L - V_{j+1}H_{j+1}^V - L_{j-1}H_{j-1}^L - F_j H_j^F + Q_j = 0 \qquad (15)$$

where the "*H's*" are the enthalpies of the appropriate phase.

For distillation operations the MESH equations with the modified summation equation instead of the two summation equations are solved for the *2c+3* independent variables: *2c* liquid and vapor mole fractions, x_{ij} and y_{ij} respectively, the vapor and the liquid flow rates, V_j and L_j respectively, and also the temperature (T_j).

2.2 Thermodynamic Properties

The simulation of multicomponent flash and distillation problems requires the enthalpies of each phase and the equilibrium ratios, relating the compositions of each component in any two phases at equilibrium.

The fundamental equation on which the whole concept of equilibrium is based is :

$$\mu_i^V \equiv \mu_i^L \qquad (16)$$

where μ_i^V and μ_i^L are the chemical potentials of component *i* in the two phases. In terms of the fugacity coefficients, the above can be transformed into

$$y_i \Phi_{iV} P \equiv x_i \Phi_{iL} P \qquad (17)$$

where P is the system pressure, y and x are the vapor and liquid compositions, Φ_{iV} and Φ_{iL} are the partial fugacity coefficients of the component i which can be obtained from an equation of state. These coefficients are calculated from the compressibility root obtained by solving the cubic equation of state for the respective phases (Walas, 1985).

When the equation of state cannot be used to model the liquid phase, activity coefficients are introduced and equation (17) becomes:

$$y_i \Phi_i P \equiv x_i \gamma_i f_{iL} \qquad (18)$$

where γ_i is the activity coefficient of the component i. Also, f_{iL} is the fugacity of liquid component i at the system temperature and pressure. The activity coefficients may be calculated using models such as UNIQUAC or the NRTL model (see, for example, Walas, 1985).

The equilibrium ratio, also called the K-value or the distribution coefficient, is a key quantity in the analysis of vapor-liquid equilibria. These ratios are dependent on the pressure, temperature and the compositions of the two phases. The expressions for the K-value of component i may be derived from equations (17) and (18) as

$$K_i \equiv \frac{y_i}{x_i} \equiv \frac{\Phi_{iL}}{\Phi_{iV}} \equiv \frac{\gamma_i f_{iL}}{\Phi_{iV} P} \qquad (19)$$

2.3 SOLVING THE MODEL EQUATIONS

2.3.1 Newton's Method

Newton's method is widely used for solving the nonlinear process model equations. A functional representation of the model equations is:

$$\boldsymbol{f}(\boldsymbol{x}) \equiv 0 \tag{20}$$

where $\boldsymbol{x}$ stands for the vector of independent variables (liquid and vapor flows, compositions and temperatures)

In Newton's method a linear approximation to equation (20)

$$\boldsymbol{J}_k \Delta \boldsymbol{x}_k = -f(\boldsymbol{x}_k) \tag{21}$$

where,

$$\Delta \boldsymbol{x}_k = \boldsymbol{x}_{K+1} - \boldsymbol{x}_k \tag{22}$$

is iteratively solved for $\boldsymbol{x}_{k+1}$ from the current guess $\boldsymbol{x}_k$ of the vector of variables; k is the current iteration number and $\boldsymbol{J}_k$ is the Jacobian matrix with elements containing the partial derivatives of f with respect to the independent variables x.

$$\boldsymbol{J}_{ij} = \frac{\delta f_i}{\delta x_j} \tag{23}$$

The convergence criterion requires the satisfaction of either of the following criteria:

$$\sqrt{\sum_{j=1}^{n}\sum_{i=1}^{e_j} f_{ij}^2} \; < \epsilon \qquad (24)$$

$$\sum_{j=1}^{n}\sum_{i=1}^{e_j} \frac{|\Delta x_{ij}|}{x_{ij}} \; < \epsilon \qquad (25)$$

where n is the number of stages, e_j is the number of equations for the j-th stage and ϵ is a small number.

Newton's method requires the calculation of the partial derivatives of all the equations involving the thermodynamic properties with respect to their variables. Most of these derivatives are obtained analytically. Composition derivatives are calculated with respect to unconstrained mole fractions (Taylor and Kooijman, 1991).

Some modifications to Newton's method are used to assist convergence.

(i) In flash calculations the K-value composition derivatives are neglected in the Jacobian matrix until the function vector falls to a value below 0.001 so that the iterations don't take any wild steps,

(ii) mole fractions that would go outside the range from 0 to 1 are limited to half of the step that would take them to the boundary,

(iii) the temperature steps are limited to 10 K and the flow changes to 50% of the absolute value of the flow itself.

2.3.2 Solving the Cubic Equation of State

Most equations of state are explicit in pressure and of the third degree

in volume in their simplest forms. Several recent papers have discussed generalized forms of cubic equations of state. Some of these cubic equations have only two parameters such as the Soave-Redlich-Kwong or the Peng-Robinson while others with three or more parameters have been proposed for better approximations of certain kinds of data. The most general representation of a cubic equation of state as a function of the compressibility (Z) is:

$$F(Z) \equiv Z^3 + f_1(A,B)Z^2 + f_2(A,B)Z + f_3(A,B) = 0 \qquad (26)$$

Here f_1, f_2 and f_3 are constant functions of A and B, the equation of state parameters. The cubic equation, when solved, has three roots. It is usually fairly simple to compute these roots for all temperatures. During a series of flowsheet calculations it is necessary to decide immediately to which phase the computed root belongs. When the mixture is operated well within the two phase region, i.e. between the bubble and dew points of the mixture the three roots obtained are all real and positive. The root with the largest magnitude is assigned as the vapor root while the one with the least magnitude is assigned as the liquid root. The intermediate root is considered to have no physical significance. At the critical point all three roots are the same. When the region of operation is below the bubble point or above the dew point, only a single real root is obtained with the other two roots being complex conjugates. To compute the roots of Equation (26) we have used a modification of the method

proposed by Gosset et al. (1985) to solve the equation of state. The algorithm can be written as follows:

Step 1:

Start with $Z = B + (0,0.1)$ to seek a liquid solution

Start with $Z = max(B,1) + (0,0.1)$ to seek a vapor solution

Step 2:

Compute the change in compressibility from

$$DZ = \frac{F(Z)}{F^1(Z)} \tag{27}$$

where $F^1(Z)$ is the derivative of F with respect to Z

Step 3:

$Z = max(Z\text{-}DZ, B)$

Step 4:

If DZ / Z is very small, assume convergence has taken place, otherwise go to step 2.

One of the problems not addressed by the above algorithm is what happens when the magnitude of the compressibility root falls below that of B, an equation of state parameter. In Gosset's algorithm no root is assigned to the phase in question and the method fails. The two possibilities under such circumstances are either that there is no solution or the algorithm has been

unable to find it even if one existed. These are cases that have not been explored before.

2.4 INITIAL ESTIMATES

Newton's method can be sensitive to the quality of the initial values and often requires initial values near the solution region. While Newton's method is powerful technique for solving problems involving nonideal mixtures, it is necessary to use care when developing the initial values. The method used to estimate the initial guesses is described in detail below.

2.4.1 Initial Estimates for Flash Calculations

In the past, failures in flash calculations when cubic equations of state were used to estimate equilibrium K-values were due to two main deficiencies (Gundersen, 1982). One was the problem of providing a reasonably good initial estimate of the phase compositions at high pressure. The other was that the commonly used methods for solving the cubic equation in compressibility sometimes leads to the wrong "type" of root being assigned to the phases. We describe in the following section a reasonably reliable method of providing the initial estimate for the flash operation as a way of tackling the former problem, while the latter problem is discussed in Chapter 3. The systematic method provided is independent of the type of flash operation performed.

The steps involved in the initialization for flash problems with the feed composition z_i are :

(i) K-values are found initially from Wilson's model (Prausnitz, 1987).

(ii) Initialization of the vapor fraction is done by the method proposed by O'Hanomah and Thompson (1984), i.e. from the various values of the Rachford-Rice function, F as a function of the vapor fraction Φ :

$$F(\Phi) \equiv \sum_{i=1}^{C} \frac{z_i(1-K_i)}{1-\Phi+\Phi K_i} \qquad (28)$$

If F(0) < 0, Φ = 0 or a subcooled liquid

If F(0) > 1, Φ = 1 or a super heated vapor

If

$$F(\Phi) = \frac{F[1/2]}{F(1/2)-F(0)} \rangle 0 \qquad (29)$$

then $\Phi = (1 - F) / 2$

or

$$\Phi = \frac{F(1/2)-0.5F(1)}{F(1/2)-F(1)} \qquad (30)$$

(iii) Liquid and vapor mole fractions are calculated from the component material balances and equilibrium equations.

2.4.2 Initial Estimates for Distillation calculations

It is imperative to develop an initialization procedure that not only reflects the physical nature of the problem but also is quite independent of the type of distillation and at the same time is efficient and inexpensive. The procedure followed in initializing distillation calculations includes the following

steps:

(i) Assumption of a constant temperature profile for all stages.

(ii) Calculation of initial K-values using Wilson's ideal solution model for all components.

(iii) Estimation of the vapor and liquid flow rates for each stage from the total material balance assuming constant molar flows with change only on the introduction of feed or the removal of the product. The condenser is taken as the first stage while reboiler as the last stage.

(iv) Determination of liquid mole fractions with the initial estimates of the K-values,the liquid and vapor flow rates by solving the component mass balances. A tridiagonal matrix equation of the form

$$[ABC]\,(x) = (R) \tag{31}$$

is solved for each component. Here,

$A_j = L_{j-1}$ form the subdiagonal matrix elements,

$B_j = -(W_j + V_j)\,K_{ij} - (U_j + L_j)$ form the diagonal matrix elements,

$C_j = V_{j+1}\,K_{i,j+1}$ form the superdiagonal matrix elements, and

$R_j = -F_j\,z_{ij}$ stand for the right hand side matrix elements.

In addition, x represents a column matrix of liquid mole fractions for component i.

(v) Normalization of the liquid mole fractions is followed by a bubble point calculation to calculate the stage temperatures and the vapor

compositions.

(vi) Steps (iv) and (v) are repeated twice and then two more times with the proper thermodynamic model.

3 COMPLEX FLASH AND DISTILLATION CALCULATIONS

The phrase complex distillation is common in the literature where it portrays distillation columns with multiple feeds, sidestreams, pumparounds and side strippers. In this chapter "complex distillation" refers to distillation calculations carried out in the complex domain. A brief discussion of some of the issues involved in carrying out complex calculations is followed by several examples of flash and distillation calculations carried out in the complex domain.

3.1 COMPLEXIFYING THE FORTRAN CODE

We had available Fortran routines for solving flash and distillation problems. The existing code is part of the software system ChemSep (Kooijman and Taylor, 1992). A necessary first step for this project involved the complexification of their code. This task went as follows: All the real variables and constants were implicitly declared to be complex double precision at the beginning of every routine, while the intrinsic functions such as DEXP, DABS, DSQRT, DLOG etc. are replaced by their complex equivalent CDEXP, CDABS, CDSQRT, CDLOG etc. respectively.

Complex constants, complex variables, complex array elements etc. may be used freely as operands in complex arithmetic expressions. Operands of different types may also be combined using the operators +, -, *, / and ** with an important exception that an operand of the type COMPLEX is never combined with an operand of the type DOUBLE PRECISION. The most difficult

part of the conversion is handling a comparison between two complex variables. The complex operands recognize only two types of relational operators namely .EQ. and .NE.. In cases where other types of relational operators are employed, either the modulus of the complex variable or only the real part of the complex variable is compared. Remembering that a complex value is merely a pair of real values makes the formatting of the input and output of complex values fairly straightforward.

3.1.1 Complexification of Variables

If all variables remain real, the iterations cannot enter the complex domain and the iterations proceed with all complex parts identically equal to zero. On obtaining the real values of the initial guesses, some of these variables are complexifed (by adding a complex contribution) to initialize the calculations in the complex domain. In the flash problems the liquid compositions of some selected components were assigned complex contributions ranging between -0.1 to 0.1. For the distillation problems, the temperatures of a few stages were given complex initial values. The complex starting points were forced to satisfy the process model equations. For example, the summation equations require the imaginary parts of the phase compositions to equal zero at the solution. Similarly, for the real valued total feed flows the imaginary parts of the total vapor and liquid should also sum to zero. With the initial guesses thus made, the model equations are solved using

Newton's method.

Another aspect of working in the complex domain is associated with the removal of the lines and surfaces of non differentiability imposed by restrictions to the real domain (Lucia et al., 1993). Also, the Cauchy-Riemann differentiability is preserved near the phase boundaries (Lucia and Xu, 1992; Lucia and Taylor, 1992). Limiting the temperature and composition variables is unimportant in the complex domain. For example, it is no longer necessary to bound the mole fractions between zero and one to prevent failure in routines that use natural logarithms in the calculation of physical properties.

The advantages of working in the complex plane will be illustrated in the examples for both flash and distillation operations that follow.

3.2 FLASH EXAMPLES

Gundersen (1982) and a few others have pointed out certain difficulties with regard to the simulation of flash operations when an equation of state is used to model the thermodynamic properties. These difficulties were discussed in Section 2.4.1. Among the two main problems that were mentioned, one concerned the assignment of the "wrong" type of root to a particular phase. This is a serious problem for mixtures being flashed near their critical point. The following examples illustrate some of the features of carrying out flash calculations in the complex domain.

Lucia and Taylor (1992) discussed the practical ramifications of using

complex-valued variables in the context of flash calculations. One of the examples they studied was a TP flash problem of an eight component mixture near its critical point (Gundersen, 1982). Poor initial guesses resulting in a Jacobian matrix that is nearly singular were chosen. The real domain calculations were found to yield a trivial solution while, on the other hand, complex-valued starting points gave a nontrivial two-phase solution with a vapor fraction between 0 to 1. Complex iterations were started by arbitrarily setting the liquid phase compositions of two components to be complex. In this section another example to study the types of variables to be complexified is considered.

3.2.1 TP Flash

A seven component purely hydrocarbon mixture is flashed at constant temperature and pressure. Three cases of the same mixture were investigated. The cases differ in the component with the highest mole fraction and the conditions of the flash, in particular the pressure as shown in Table 3.1.

Trivial solutions were obtained in all cases with real starting points generated by the procedure discussed in Chapter 2 due to the conditions being near the critical region of the respective mixtures. We investigated the convergence characteristics of the problem when different variables were provided complex initial values.

Significant complex parts were added to the initial compositions of the components in different combinations. The simulation then proceeded in the

Table 3.1 TP Flash Problem

INLET FEED CONDITIONS :

Components	Inlet Flow (kmol / h)		
	Case 1	Case 2	Case 3
Methane	0.943	0.1	0.05
Ethane	0.027	0.7	0.1
Propane	0.0074	0.03	0.7
n-Butane	0.0049	0.06	0.03
n-Pentane	0.0027	0.05	0.06
Nitrogen	0.014	0.05	0.01
n-Hexane	0.001	0.01	0.05
Temperature (°C)	-70.02	-70.02	-70.02
Pressure (atm)	58.11	161.5	256.5

Table 3.2 Solution to TP Flash Problem

SOLUTION :

Components	K - Values		
	Case 1	Case 2	Case 3
Methane	(1.066,3.72E-09)	(0.987,-2.12E-07)	(0.967,3.68E-09)
Ethane	(0.899,-7.28E-08)	(0.511,-5.8E-09)	(0.42,9.8E-10)
Propane	(0.826,-1.25E-07)	(0.326,6.08E-08)	(0.244,5.57E-10)
n-Butane	(0.759,-1.74E-07)	(0.209,1.15E-07)	(0.142,2.14E-10)
n-Pentane	(0.697,-2.1E-07)	(0.135,1.48E-07)	(0.0853,2.46E-11)
Nitrogen	(1.069,4.72E-08)	(1.455,-6.07E-07)	(1.617,1.34E-08)
n-Hexane	(0.64,-2.59E-07)	(0.088,1.62E-07)	(0.052,-7.48E-11)

complex domain. The solutions to all three cases are shown in Table 3.2. These solutions were found from starting points with widely varying complex magnitudes. It can seen from the solutions that the imaginary parts of the K-values are relatively small when compared to that of the real part and the K-value may, therefore, be considered real. Also, it was found that complexifying the component with the highest mole fraction among the components increased the chances of convergence (in 90% of the cases).

3.2.2 QP Flash

A mixture of benzene, toluene and ethylbenzene at a feed pressure of 3 atms. and 453 K is flashed at 22 atms. and zero heat duty. These conditions are near the critical point of the mixture. The Peng-Robinson equation of state was used to model the vapor and liquid phase. Solving this problem in the real domain resulted in a trivial solution after about eighteen iterations, the K values tending to one. The same problem when simulated in the complex domain with real starting points (i.e. with zero imaginary parts) easily converged to a nontrivial two phase solution in about fourteen iterations.

3.3 BIFURCATION OF ROOTS TO CUBIC EQUATION OF STATE

The behavior of the examples discussed above can be explained by the fact that the cubic equation of state yields a single real root and two complex roots especially within the two phase region near the critical point. Working in the real domain precludes the use of complex roots and hence the same real

root is assigned to both phases (according to the Gosset et al. algorithm). The composition of the vapor thus equals the composition of the liquid and the K-values approach unity (trivial solution). On the other hand, working in the complex domain enables the assignment of both real and complex roots to the appropriate phases i.e. to the vapor and liquid phase as appropriate. In those cases where a complex root is assigned to a particular phase other thermodynamic properties like the fugacity coefficients and the K-values also become complex and, henceforth, the iterations proceed in the complex domain.

Figures 3.1(a) - 3.5(c) displays roots of the SRK equation of state as a function of temperature for the eight component mixture mentioned above. Each figure shows a three dimensional view as well as the projections of this view on to the real and complex planes. It can be seen that for all the reduced pressures (i.e. for Pr = 0.25, 0.75, 1.0, 1.5, 4.0) there is always one root that remains real. From the real projections at low reduced pressures such as 0.25 (Fig. 3.1a) and 0.75 (Fig. 3.2a) one can notice the two bifurcation points are located some distance apart. The three real roots lie between these bifurcation points. As the pressure is increased the distance between the bifurcation points decreases and when Pr =1, the bifurcation points coincide (Fig. 3.3) with three repeated real roots existing at this point. Any further increase in pressure say to Pr = 1.5 (Fig. 3.4) or Pr = 4 (Fig. 3.5) no more bifurcation occurs and from the complex projections at these pressures, it is evident that the

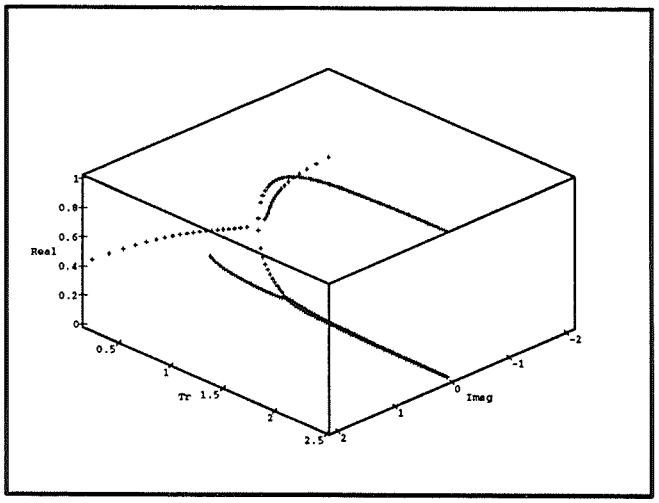

(a) 3D View

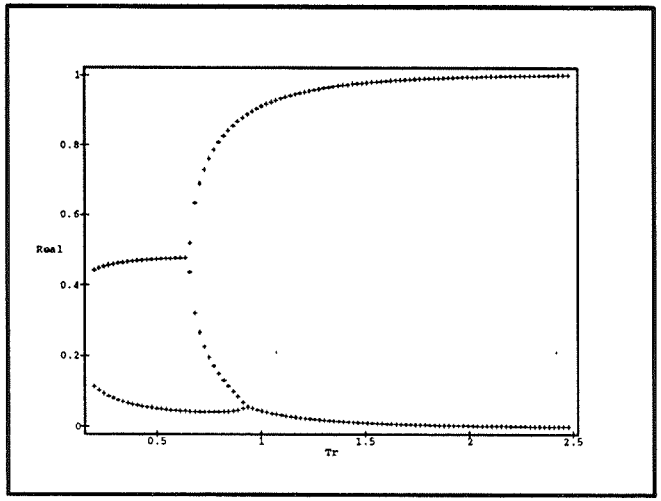

(b) Real Projection

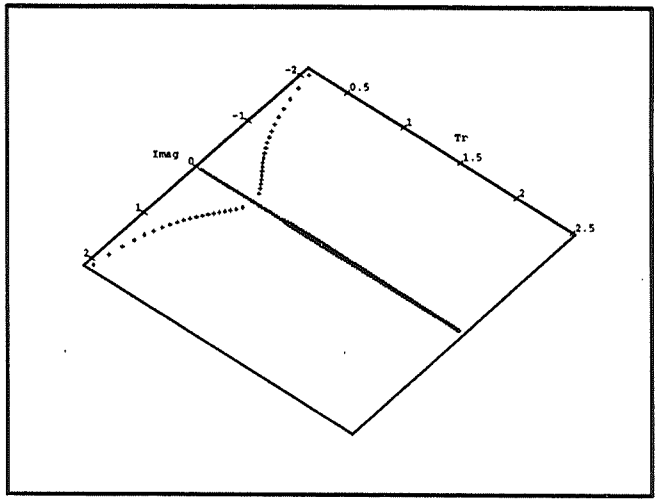

(c) Complex Projection

Figure 3.1 Bifurcation of Compressibility roots to SRK equation at Pr = 0.25

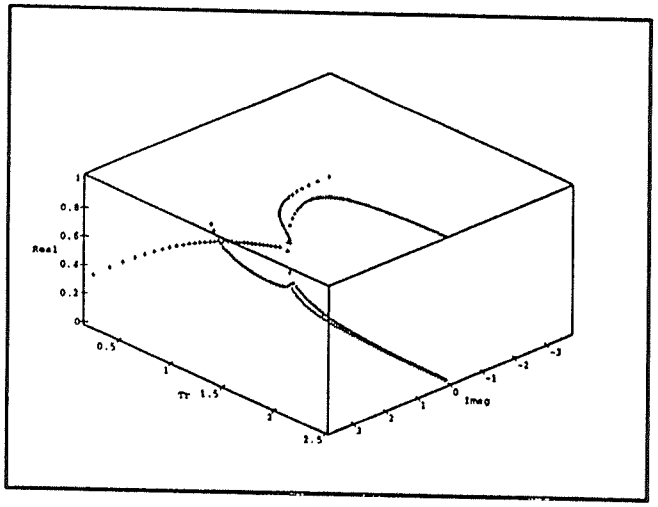

(a) 3D View

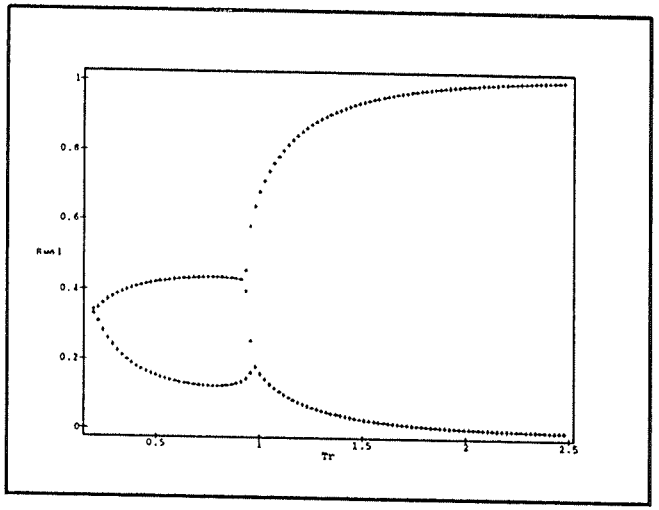

(b) Real Projection

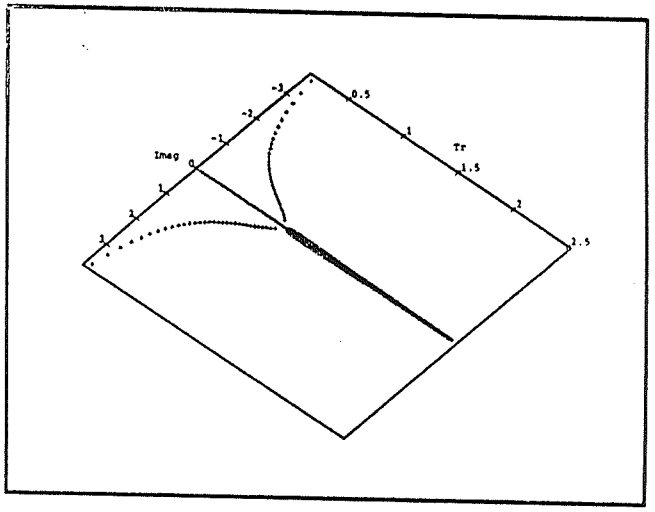

(c) Complex Projection

Figure 3.2 Bifurcation of Compressibility roots to SRK equation at Pr = 0.75

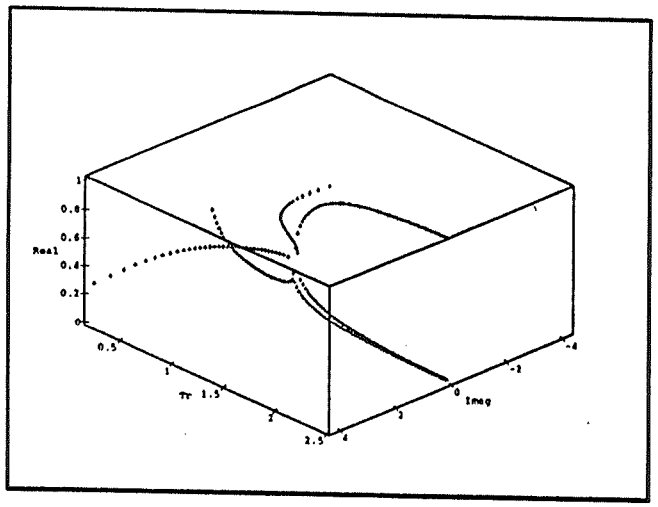

(a) 3D View

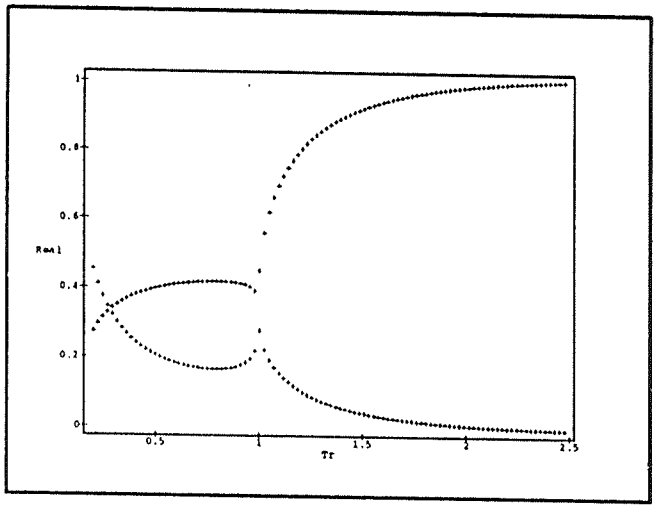

(b) Real Projection

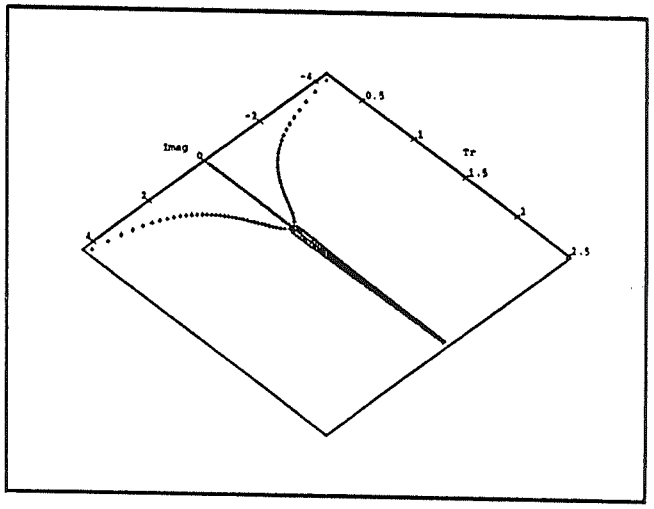

(c) Complex Projection

Figure 3.3 Bifurcation of Compressibility roots to SRK equation at Pr = 1.0

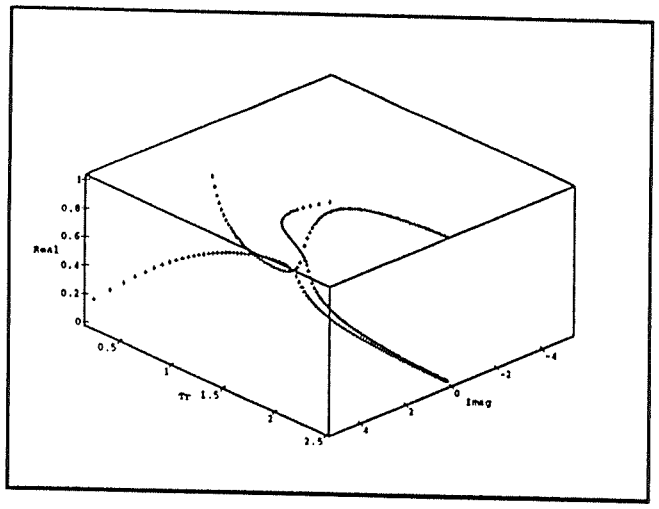

(a) 3D View

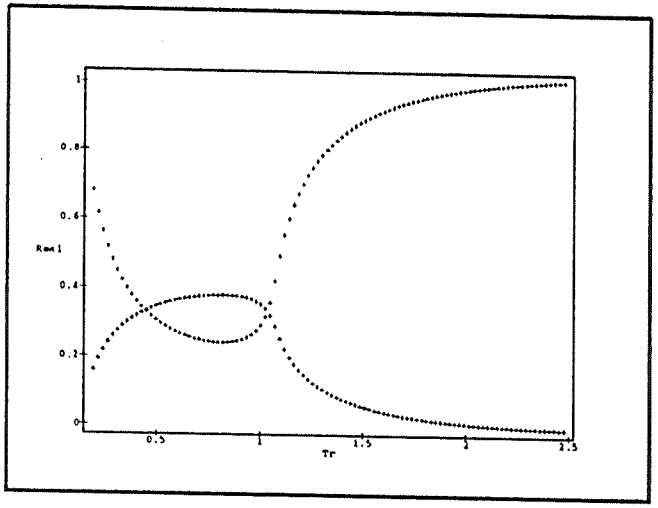

(b) Real Projection

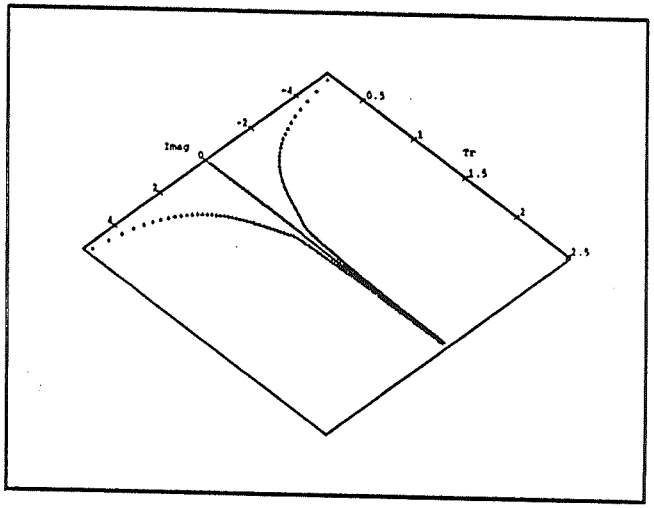

(c) Complex Projection

Figure 3.4 Bifurcation of Compressibility roots to SRK equation at Pr = 1.5

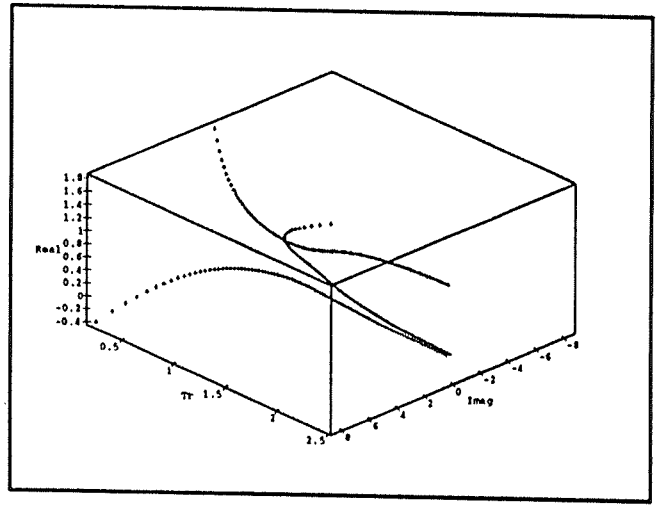

(a) 3D View

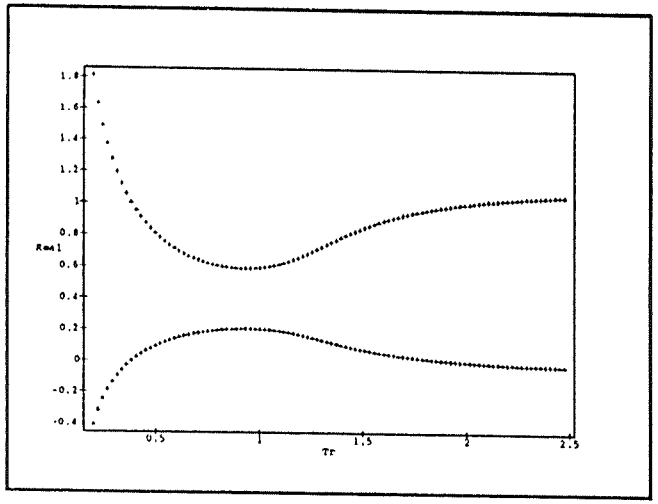

(b) Real Projection

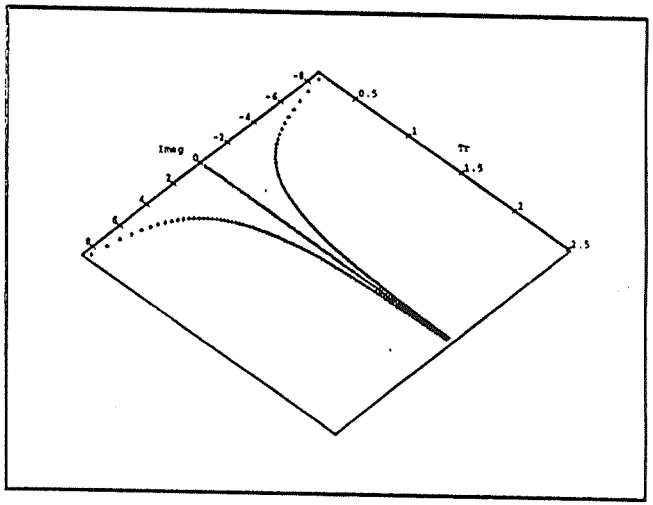

(c) Complex Projection

Figure 3.5 Bifurcation of the Compressibility roots to SRK equation at Pr = 4.0

imaginary roots asymptotically approach to the real axis at $T = \infty$.

In the neighborhoods of the regions where both Tr and Pr are both less than 1, i.e. within two phase envelope, the conventional real domain calculations assign the single real root to any phase and thus the calculations are led to a trivial solution. On the other hand, in the complex domain calculations, a complex root may be assignable to any particular phase.

What is even more surprising is the fact that in spite of the fact that the simulation take place in the complex domain, the solution obtained after only a modest number of iterations is real with negligible imaginary parts.

It can be concluded that nontrivial real solutions for specifications in the two phase region can be easily found using complex-valued starting points.

3.4 MULTISTAGE SEPARATION PROCESSES

In the following sections we study a few examples of multistage operations that are commonly difficult to simulate either due to their sensitivity to the specified parameters or to their complicated solution structures. All mathematical calculations are performed in both the real and complex domains. Figures illustrating some of the results obtained with this new approach are also presented.

3.4.1 Reboiled Absorber

In this example, which represents an actual column, a nine component mixture containing mostly hydrocarbons of widely ranging boiling points is separated. The operation is carried out in a ten stage column having a partial reboiler and no condenser with the feed introduced at the first stage as shown in Fig. 3.6. The top and bottom pressures are specified. The bottoms specification is the mole fraction of methane (mole fraction = 0.009). The Peng-Robinson equation of state is used to model the vapor and liquid phases with appropriate interaction parameters.

This is a very difficult problem to solve since the column is operating close to the critical point of the mixture at some point inside the column. As noted earlier, flash calculations near the vicinity of the critical point can be difficult to convergence and this difficulty is expected to carry over to column simulations. In addition, the problem is extremely sensitive to the bottoms product specification; varying the mole fraction of methane, even slightly, led to aperiodic behavior with the real domain calculations failing to converge. This behavior was observed for several values of the bottoms specification.

This particular problem is easy to solve using the complex code. On initializing the process variables in the form of complex numbers, with a few of them being assigned appreciable imaginary parts, a real solution (i.e. with negligible imaginary parts) was obtained in a modest number of iterations. The profiles for the liquid and vapor flows and also the K-values at the solution for

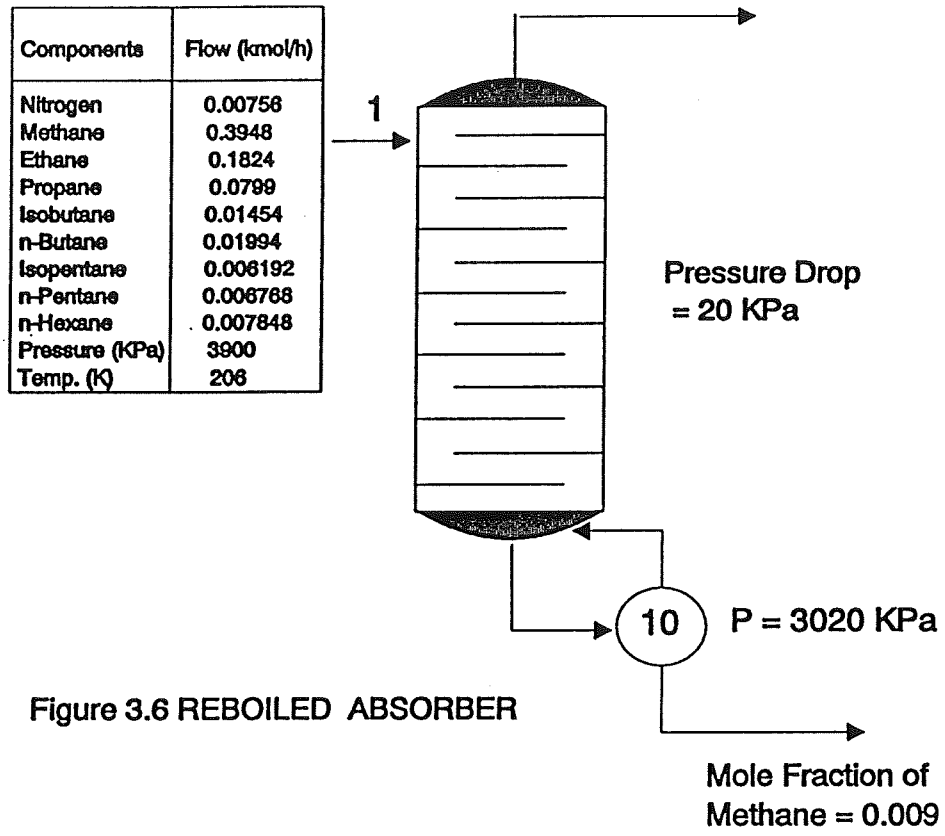

Figure 3.6 REBOILED ABSORBER

Table 3.3 Stream Data for Reboiled Absorber

Components	Top Product	Bottom Product
1. Nitrogen	(1.80E-02,-4.09E-17)	(3.75E-09, 2.50E-22)
2. Methane	(9.34E-01,-2.01E-15)	(9.03E-03, 8.66E-26)
3. Ethane	(4.42E-02, 2.04E-15)	(5.45E-01,-1.25E-15)
4. Propane	(3.46E-03, 9.24E-17)	(2.62E-01, 6.91E-16)
5. Isobutane	(1.80E-04, 4.85E-18)	(4.82E-02, 1.45E-16)
6. n-Butane	(1.59E-04, 4.44E-18)	(6.62E-02, 2.04E-16)
7. Isopentane	(1.30E-05, 4.03E-19)	(2.06E-02, 6.49E-17)
8. n-Pentane	(1.05E-05, 3.38E-19)	(2.25E-02, 7.11E-17)
9. n-hexane	(2.78E-06, 1.11E-19)	(2.61E-02, 8.29E-17)
Flow (kmol/h)	(4.19E-01, 2.65E-19)	(3.0E-01,-2.65E-19)
Temp. (K)	(200.09, 6.53E-13)	(310.71,1.06E-13)

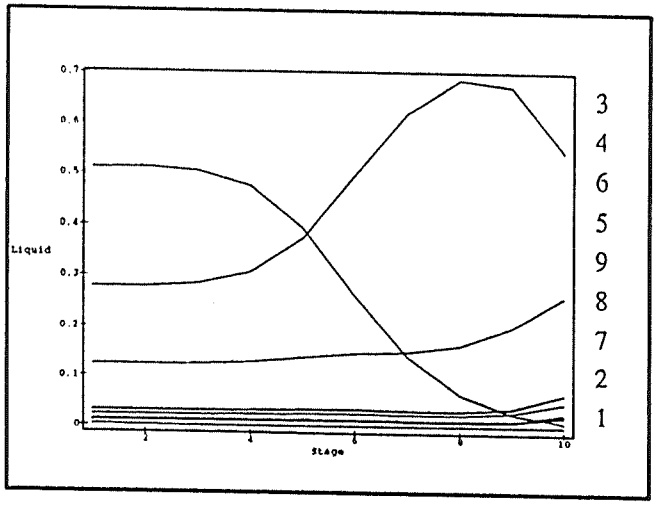

(a) Liquid Profiles

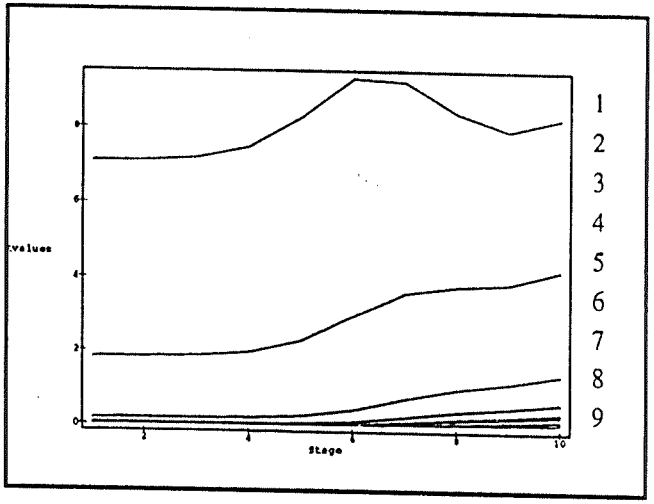

(b) K-Value Profiles

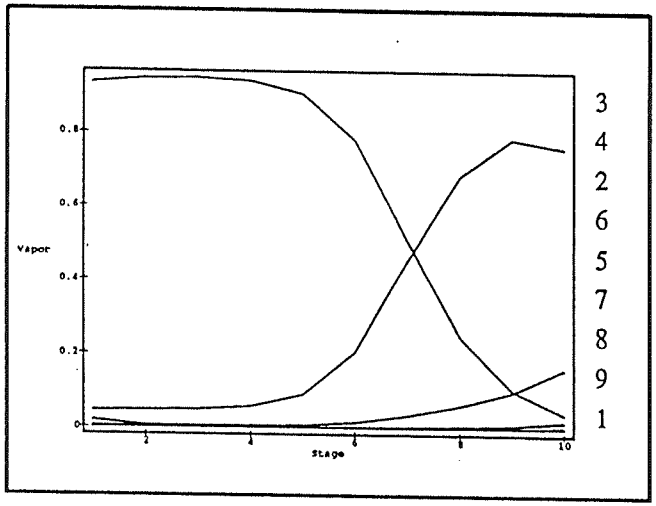

(c) Vapor Profiles

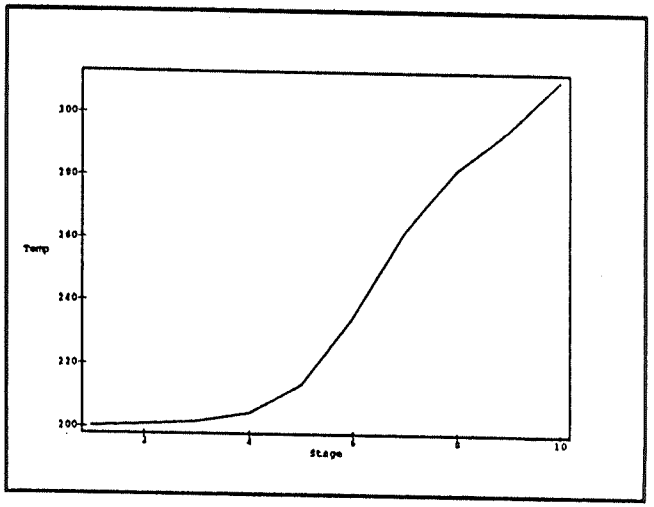

(d) Temperature Profile

Figure 3.7 Solutions to Reboiled Absorber

(Component numbering as given in Table 3.3)

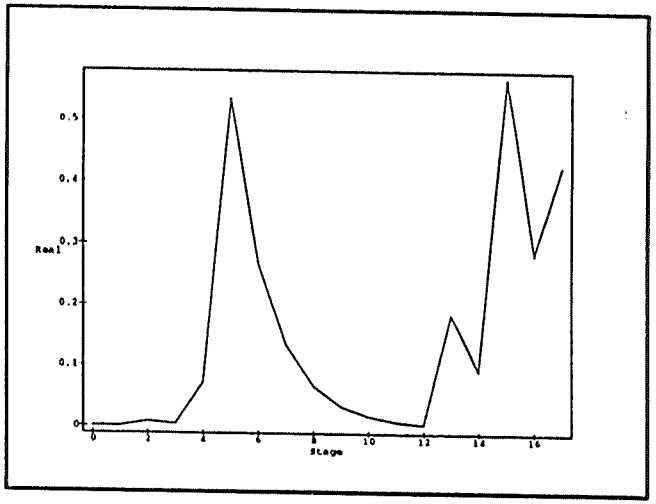

Figure 3.8 Iteration History of n-Hexane Vapor Mole fraction in Real Domain

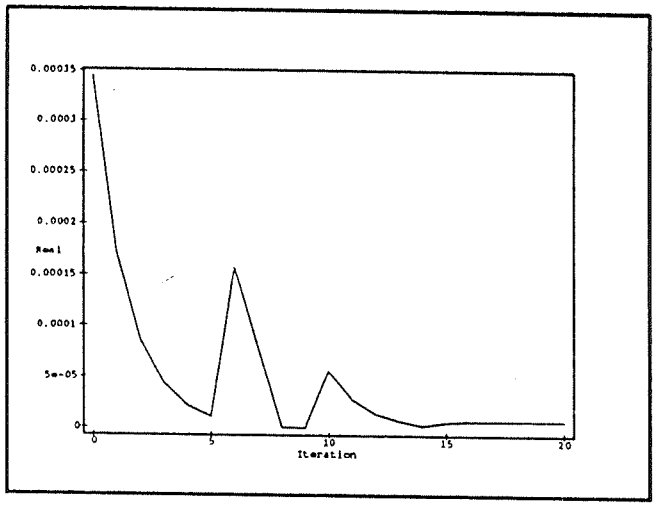

(a) Real Projection

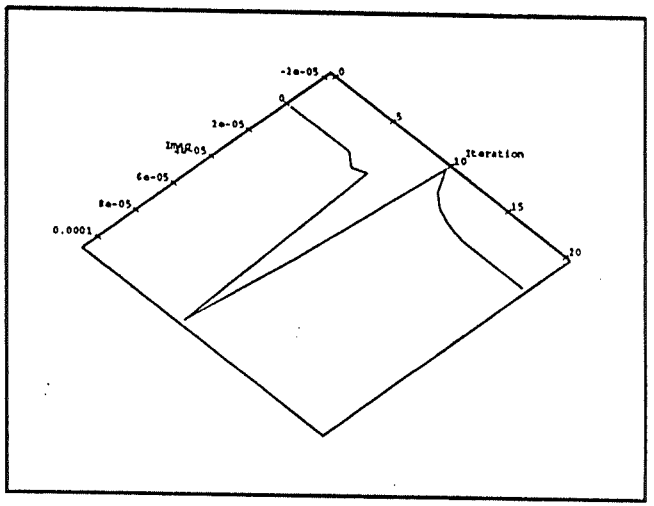

(b) Complex Projection

Figure 3.9 Iteration History of n-Hexane Vapor Mole fraction in Complex domain

REBOILED ABSORBER

the methane mole fraction specification (=0.009) are given in Figs. 3.7(a) - 3.8(d). Table 3.3 gives the stream data representing the mole fractions of all the components at the solution. Real solutions were obtained without difficulty over a wide range of bottoms specifications; i.e. for mole fractions of methane between 0.007 to 0.4. Fig 3.8 shows the path taken by the n-Hexane vapor on the fifth stage during the course of iterations in the real domain while Figs. 3.9(a) and 3.9(b) show the course of the iterations for the same variable in the complex domain. It can be seen that the calculations take wide steps into the complex domain before converging to a real solution.

3.4.2 Liquified Natural Gas Plant

Similar behavior was also found with an example of a Liquified Natural Gas (LNG) plant adapted from a paper by Christiansen et al. (1979) in which Naphtali-Sandholm distillation calculations were performed to model the separation of natural gas mixtures near the critical point. In their paper a mixture containing saturated hydrocarbons ranging from methane to heptane was the feed to a plant consisting of a demethanizer, depropanizer, deethanizer and debutanizer. Thermodynamic properties were calculated from the Soave-Redlich-Kwong equation of state. In the calculation of the roots of the compressibility polynomial the root was assigned to be liquid if the compressibility was lesser than 1/3 and to the vapor phase if the compressibility factor were greater than 1/3. If the iterations resulted in a phase not meeting these requirements, the phase was considered

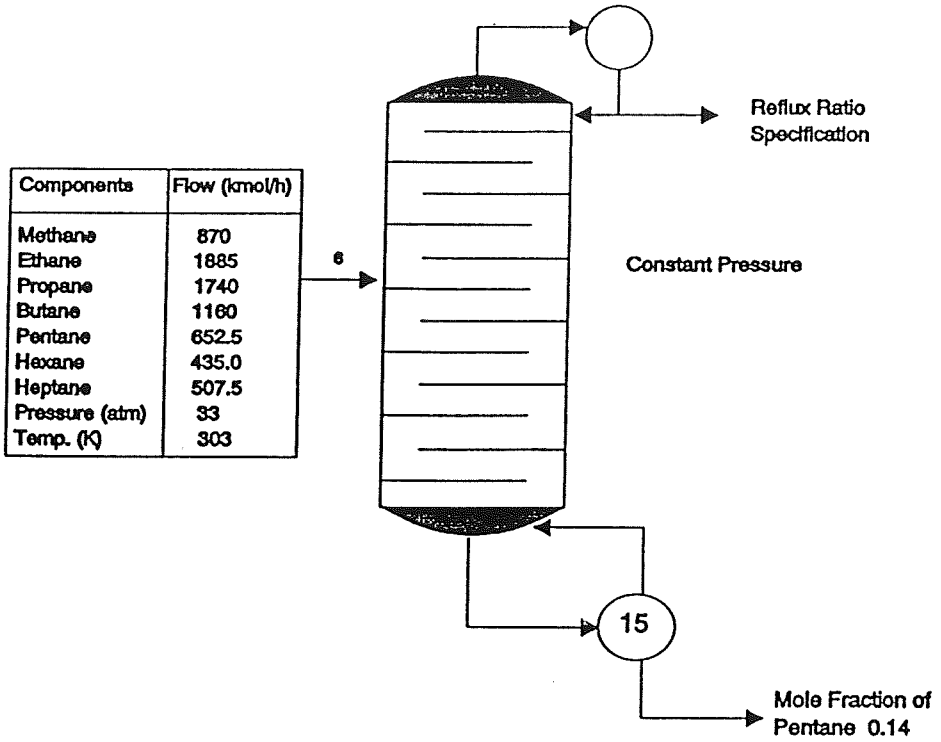

Figure 3.10 DEMETHANIZER

Table 3.4 Stream Data for Demethanizer

Components	Top Product	Bottom Product
1. Methane	(3.36E-01,-1.66E-23)	(6.10E01, 3.47E-24)
2. Ethane	(6.64E-01, 1.00E-18)	(3.55E-02,-5.58E-19)
3. Propane	(3.75E-05,-1.0E-18)	(3.73E-01, 5.58E-19)
4. Butane	(1.46E-08,-8.72E-22)	(2.48E-01, 4.88E-22)
5. Pentane	(5.80E-12,-5.54E-25)	(1.48E-01, 1.96E-24)
6. Hexane	(4.95E-14,-6.56E-28)	(9.33E-02, 1.38E-24)
7. Heptane	(2.80E-18,-4.77E-31)	(1.08E-01, 1.58E-24)
Flow (kmol/h)	(2588.4, 1.817E-23)	(4658.4,-1.79E-23)
Temp. (K)	(246.85, 5.24E-13)	(364.91,8.82E-17)

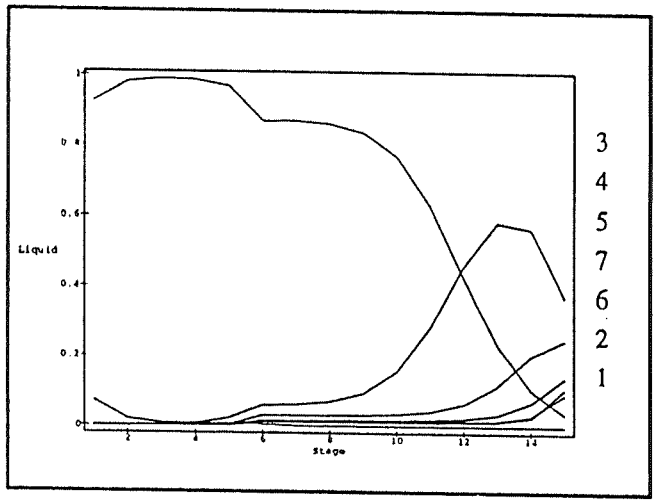

(a) Liquid Profiles

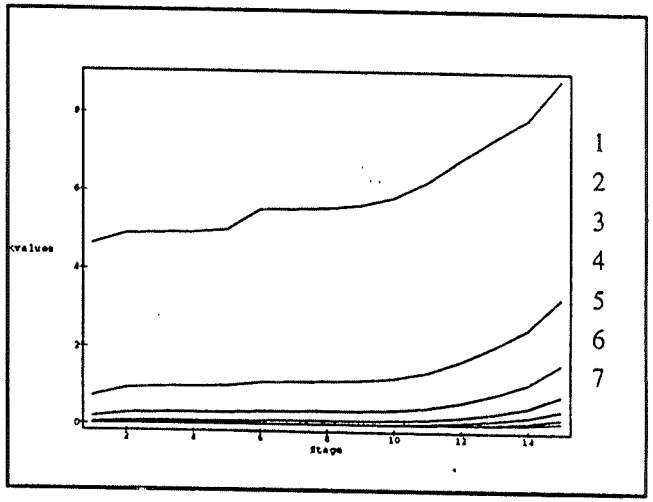

(b) K-Value Profiles

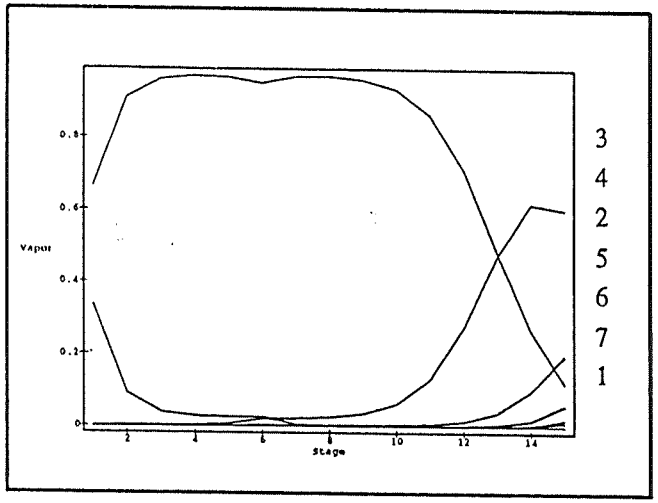

(c) Vapor Profiles

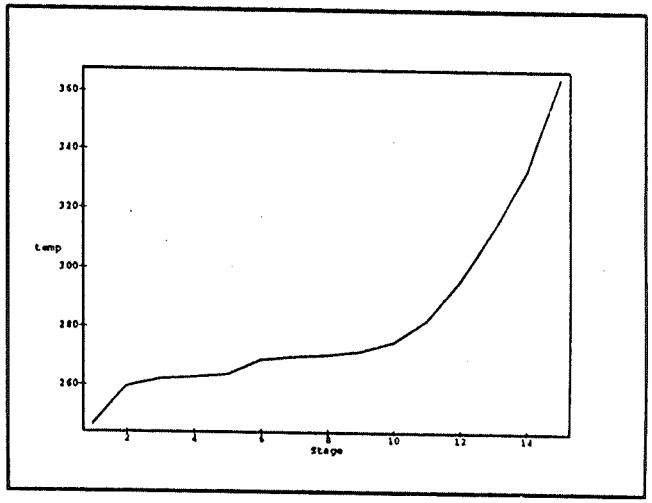

(d) Temperature Profiles

Figure 3.11 Solutions to Demethanizer

(Component numbering as given in Table 3.4)

hypothetical and the temperature changed to a level where both phases existed.

Here we consider the demethanizer alone, specifications for which are given in Fig. 3.10. The conditions are near the critical region of the distillate which is mostly methane and ethane. When the reflux ratio is given as the top specification and the purity of a component is given as the bottoms specification, the real-domain calculations failed to converge to a solution. On the other hand, the complex code was able to find the real-valued solutions for a range of bottoms specification. The profiles at the solution for the bottoms specification of n-pentane mole fraction (=0.14) are shown in Figs. 3.11(a)-(d).

It is evident from this and the preceding example and from the other equation of state examples that have been considered in Sections 3.2.1 and 3.2.2, that working in the complex plane helps in finding real solutions that are difficult or impossible to obtain while working solely in the real domain.

3.4.3 The Acetonitrile-Water-Acrylonitrile System

A problem involving acetonitrile, water, and acrylonitrile at atmospheric pressure in a two stage column as shown in Fig. 3.12(a) is considered next. The feed is introduced to the second stage. The vapor phase is assumed ideal while the liquid phase is modelled using the UNIQUAC equations.

This problem was created by Lucia et al.(1990) to study the chaotic behavior of the direct substitution method of solving equations. The boil-up ratio was fixed at 94.5 kmol/h and the distillate rate was varied between 22-32

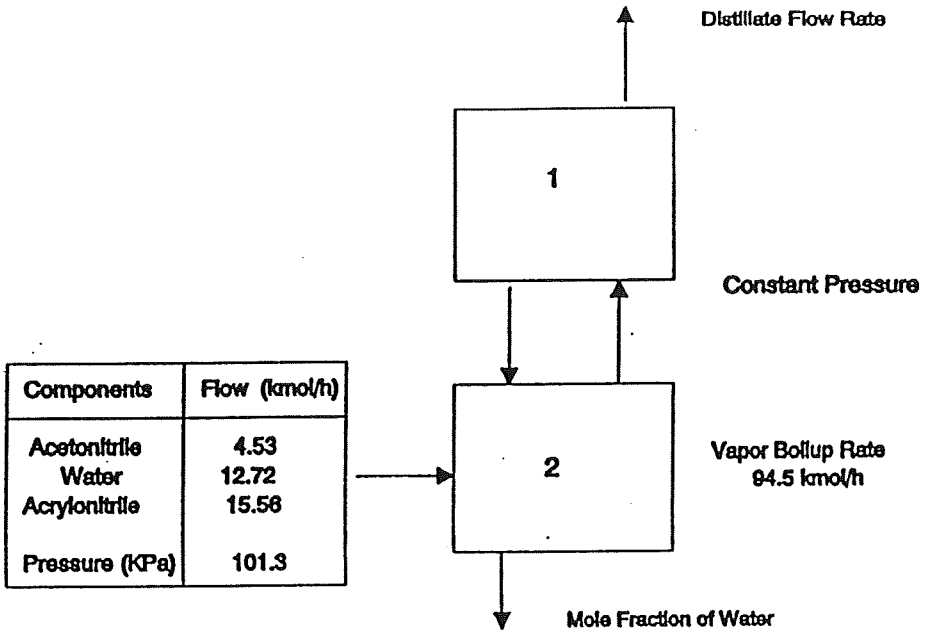

Figure 3.12 Acetonitrile-Water-Acrylonitrile

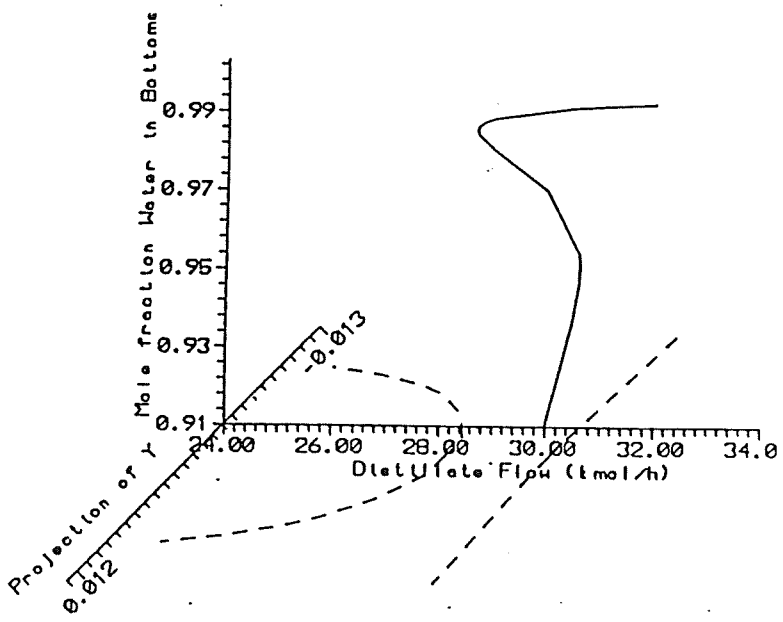

Figure 3.13 Bifurcation Diagram for Acetonitrile-Water-Acrylonitrile System

kmol/h. A combination of direct substitution and Newton's method was used to solve the problem. When parameterized in distillate flow rate Lucia et al. have shown that this problem has multiple two phase (homogeneous) solutions, as well as three-phase behavior. At various values of the distillate flow rate, transitions from convergent to nonconvergent behavior were observed. Also, due to the complicated interactions between the methods used to solve the problem, abrupt changes in periodicity and period doubling bifurcations were noticed and it was concluded that this occurred due to the multiplicity at Stage 2.

We have used Newton's method to solve all model equations at once and verified the multiplicity of real solutions as shown in Fig. 3.13. In addition, we have found multiple complex solutions very near the turning points of the multiplicity curve. The solid curve in Fig. 3.13 indicates the parameterized curve while the dashed lines indicate the contour of the complex solutions near both of the bifurcation points. When real domain calculations are performed in regions where the complex solutions exist the iterations exhibit truly bizarre behavior.

3.4.4 The Ethanol - Benzene - Water System

Azeotropic distillation is one of the most commonly used and most important separation operations in the chemical industries. Calculations for azeotropic distillation systems are considered more difficult then for simple distillation or even for extractive distillation. The complication arises from the

strongly nonideal behavior that leads to the formation of an azeotrope by the entrainer.

One of the frequently reported features of these separation processes is the existence of multiple steady state solutions to the model equations; i.e. the ability of a system to exist in more than two stable steady states under the same conditions. Multiple steady states may exist when one of variables like the distillate flow or the feed composition vary nonmonotonically along the continuation path of the bifurcation diagram. According to Kienle and Marquardt (1989), interactions between different dynamic subsystems within a system are the reasons for instability and steady-state multiplicity in many chemical systems (as well as in many other systems in science and engineering).

Along with these multiplicities the regions near the turning points are of interest due to the difficulty of converging to real solutions in the neighborhood of the turning points.

Robinson and Gilliland (1950) were among the first to study the ethanol-benzene-water system. Originally the column used to dehydrate ethanol using benzene has the overhead vapor from the column condensed to form two liquid phases that are separated in a decanter. The organic rich phase was returned to the top tray as reflux together with a portion of the water-rich phase and makeup benzene. The other portion of the water-rich phase was sent to a stripping column to recover the organic compounds. In the

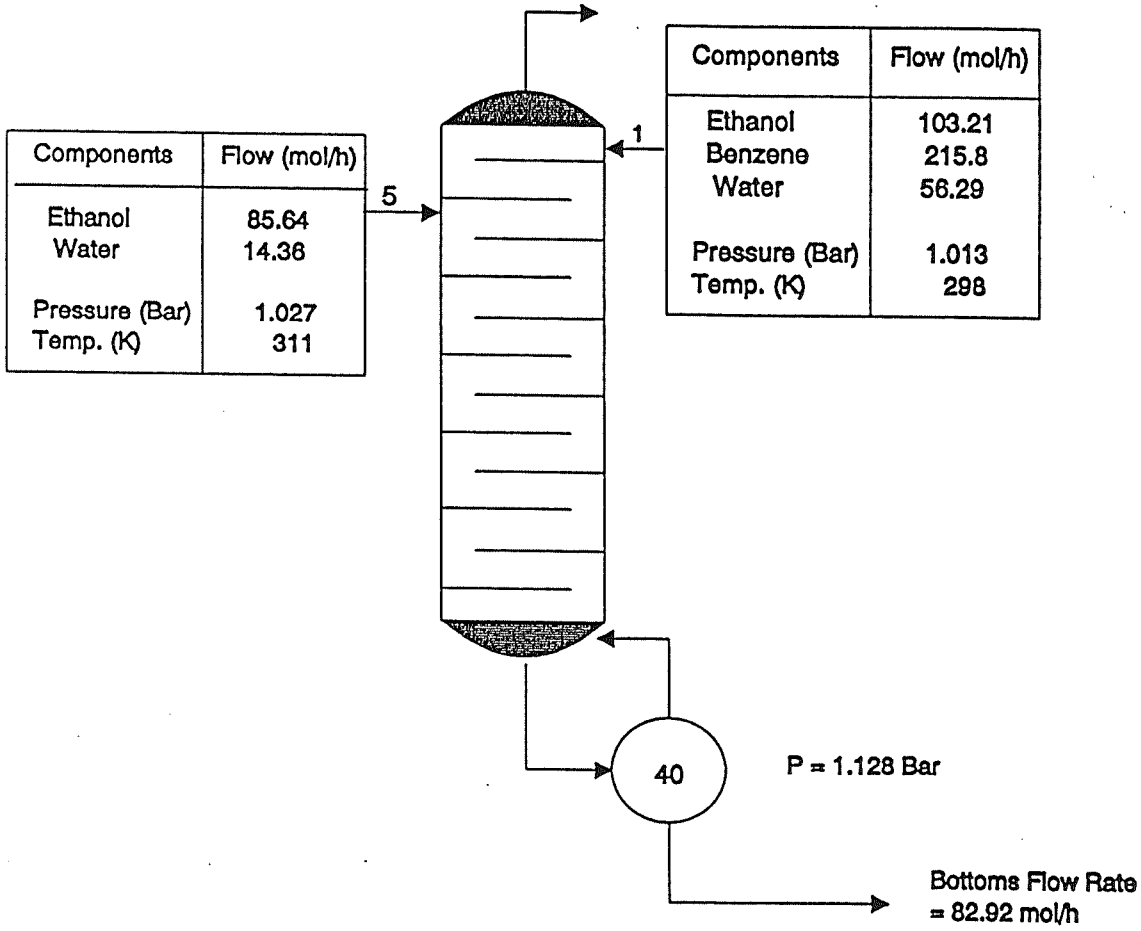

Figure 3.14 Azeotropic Distillation of Ethanol-Benzene-Water

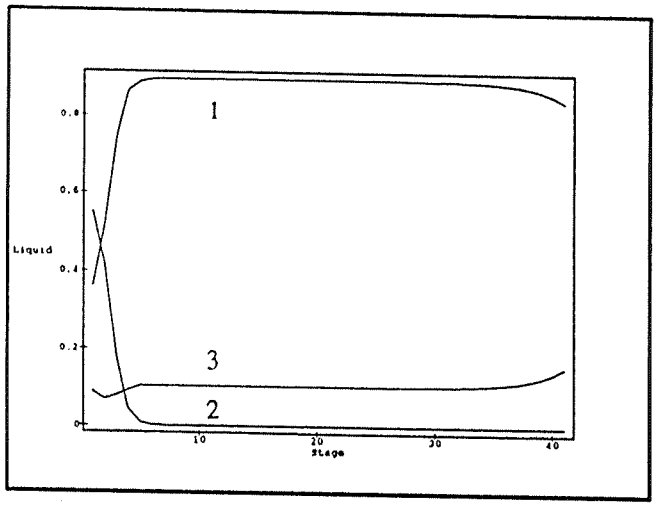

(a) Low Purity Profiles

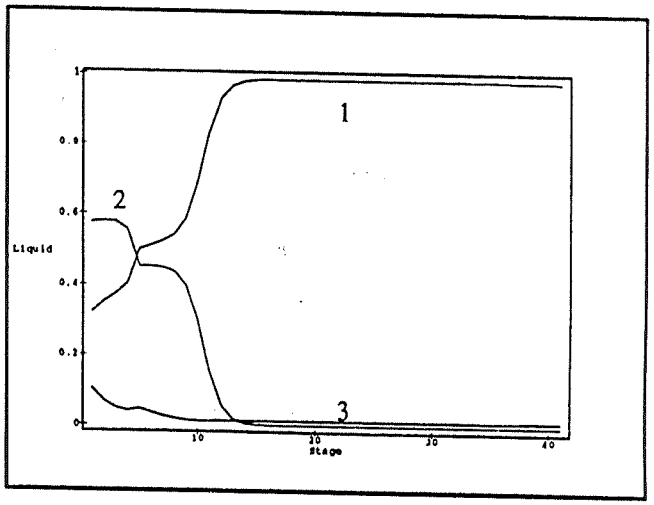

(b) Intermediate Purity Profiles

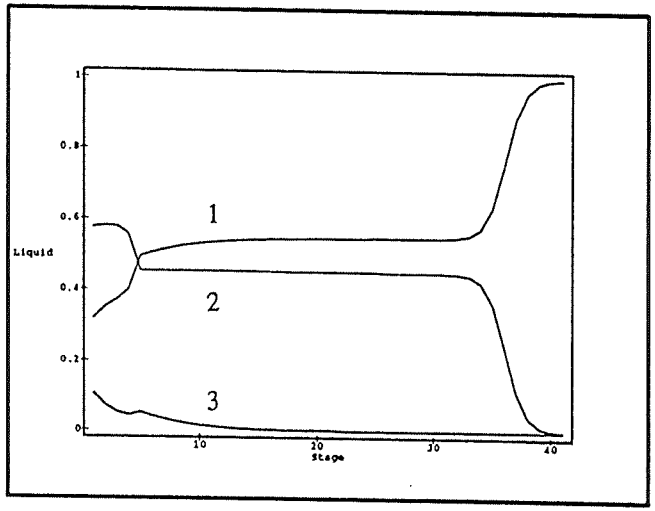

(c) High Purity Profiles

Figure 3.15 Multiple Solutions for Ethanol feed Flow of 103 kmol/h

Ethanol(1)-Benzene(2)-Water(3)

numerical studies conducted by Magnussen et.al (1979), Prokopakis and Seider (1983), Venkataraman and Lucia (1988) and Rovaglio and Doherty (1990) multiple steady state solutions were confirmed and were attributed completely to its potential heterogeneity.

In our calculations, the Prokopakis et al. column as shown in Fig. 3.14 is used with the decanter removed and a second feed introduced at the top of the column to simulate the reflux. Convergence can be difficult to obtain due to the significant dependence on the type of specification made. For an ethanol feed flow of 103 mol/h, three real solutions are found and the profiles are shown in Figs. 3.15(a)-(c). The vapor is considered to be ideal while the UNIQUAC model is used to model the liquid phase. The parameters for the activity coefficients are given by Prokopakis and Seider (1983).

The low purity profile in Fig. 3.15(a) is easiest to obtain from the standard initial estimates as described earlier. The high purity solutions are obtained from an initial profile calculated assuming the stage efficiency to be very low (0.1), and hence the composition and temperature profiles in Fig. 3.15(c) are almost flat. The intermediate profile Fig. 3.15(b) is more difficult to obtain. We were able to find it using the converged high purity solution obtained with an efficiency of 0.83 as the starting point. Fig. 3.16 shows the composition of water in the bottoms product as a function of the ethanol flow in the simulated reflux. The three solutions are seen to exist over a range of ethanol flows from about 101.8 to 103.4 mol/h. Similar S-curves are found

when the bottoms flow rate is varied, Venkataraman and Lucia (1988).

Bekiaris et al. (1992) and also Magnussen et al. (1979) believe that since the liquid composition profiles of the multiple solutions lie entirely in the single liquid phase region it is correct to conclude that the multiplicities are not due to the heterogeneity of the system. In other words, the column behaves like a homogeneous azeotropic column.

The focus of our study on this system has been around the regions at the turning points of Fig. 3.16. It has been found again, just as in the case of the previous example, that a bifurcation of the real solutions into the complex domain takes place near both of the turning points (i.e. between the transitions from the low to the intermediate purity and from the intermediate to the high purity solution).

The high and the low purity real profiles very near the turning points of the vapor and liquid compositions, the K-values and the temperatures are shown in Figs.3.17(a)-(d) and 3.18(a)-(d) respectively. The same profiles of both the high and low purity complex solutions also obtained very near the turning points are shown in figs.3.19(a) to 3.22(c) and 3.23(a) to 3.26(c) respectively. These figures include the three dimensional views of each of the profiles and their projections on the real and complex plane. The projections on to the real plane are similar to the real profiles themselves; the complex projection, on the other hand shows significant complex contributions.

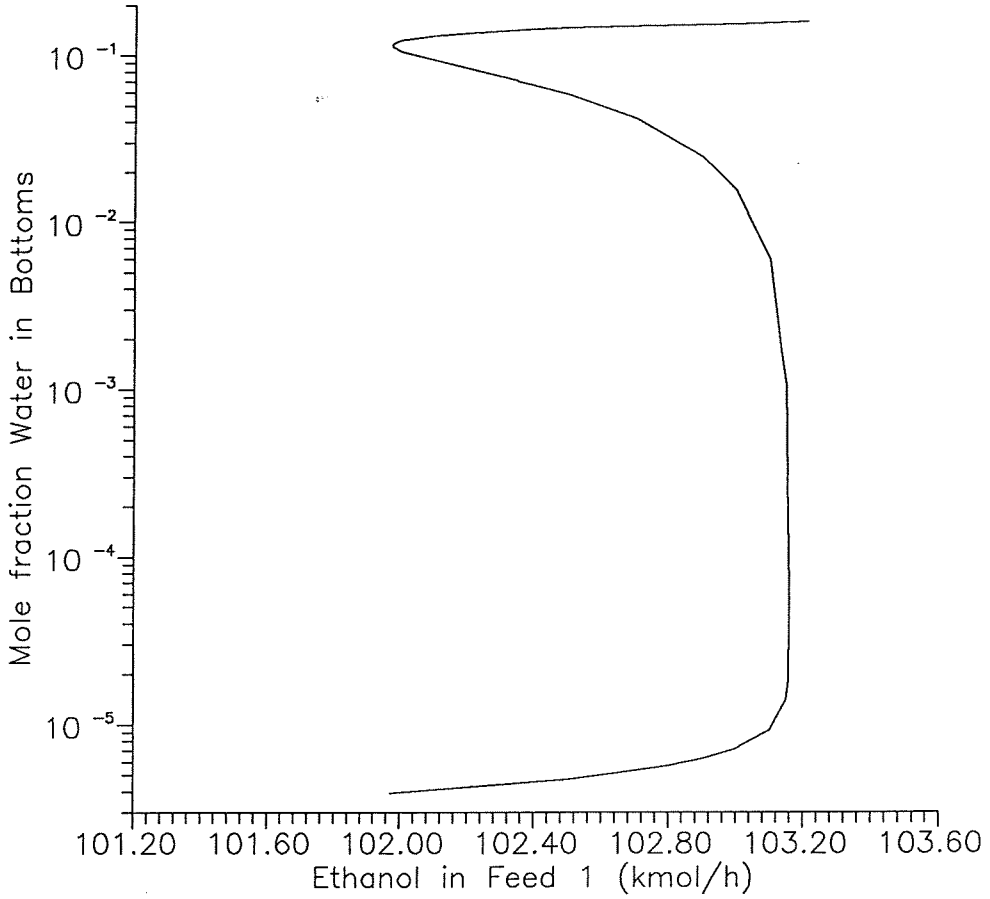

Figure 3.13 Bifurcation Diagram of Ethanol–Benzene–Water System

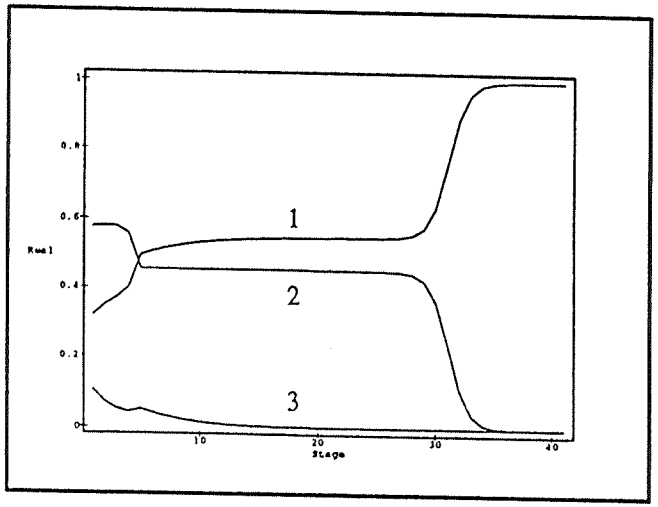

(a) Liquid Compositions

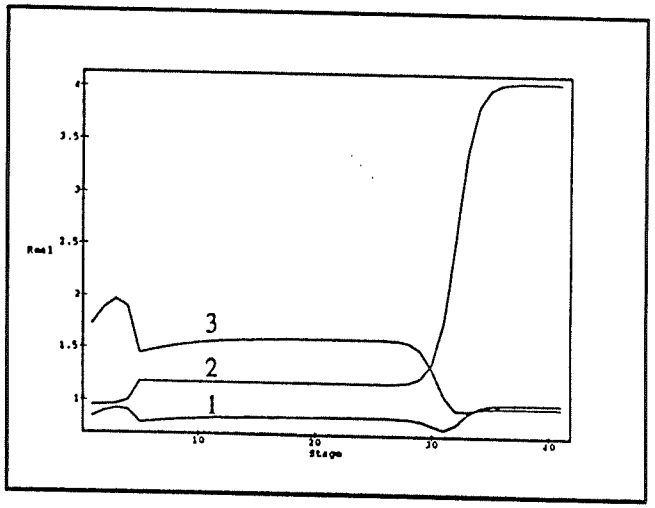

(b) K-Values

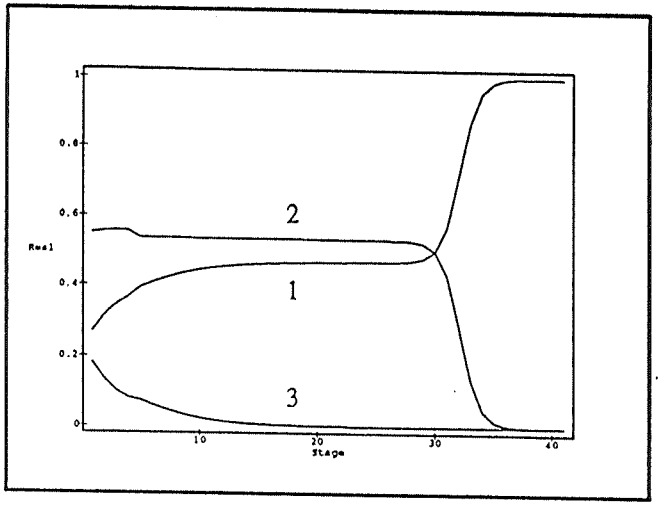

(c) Vapor Compositions

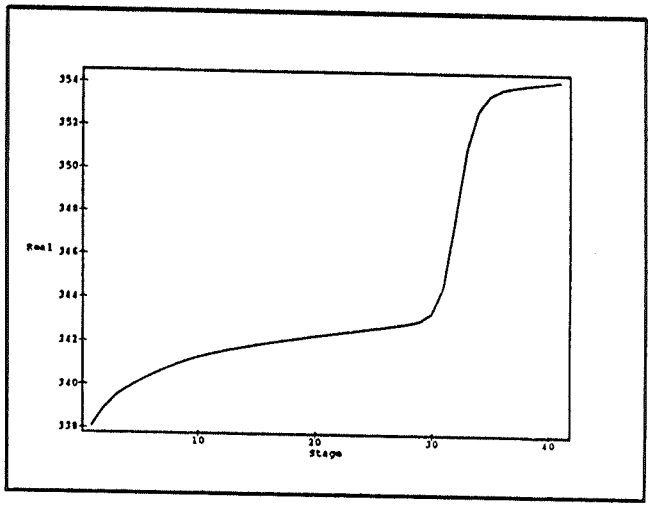

(d) Temperature Profile

Figure 3.17 High Purity Real Solutions

Ethanol(1)-Benzene(2)-Water(3)

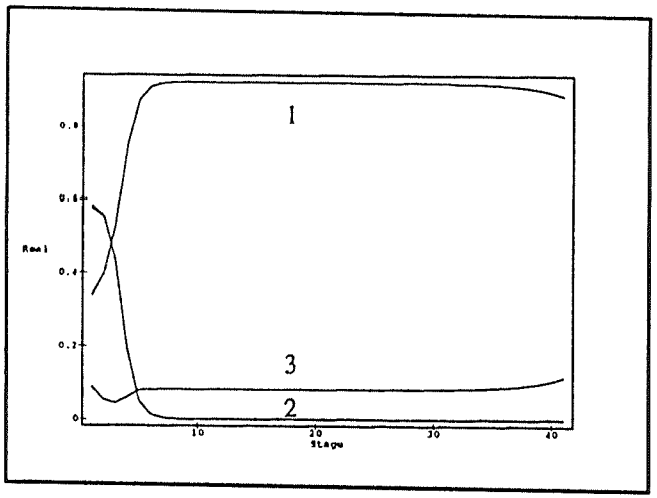

(a) Liquid Compositions

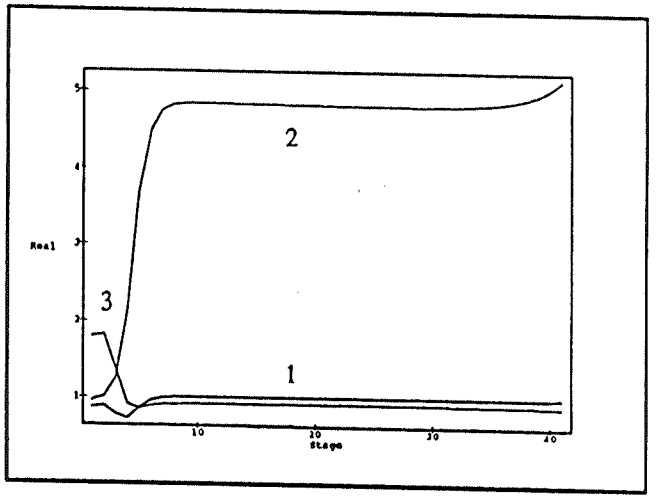

(b) K-Values

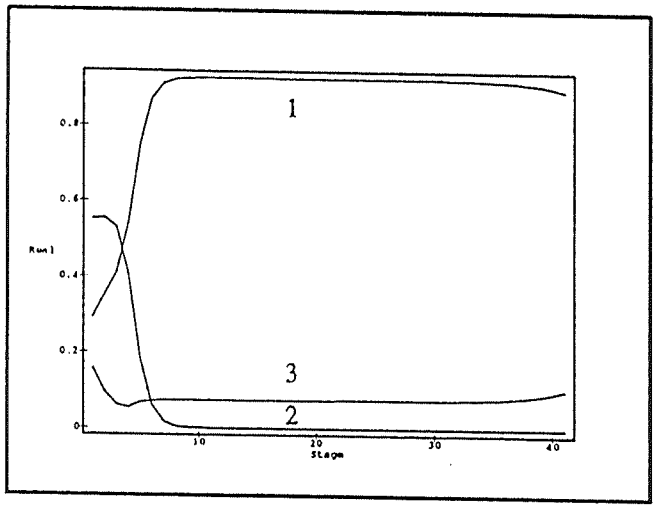

(c) Vapor Compositions

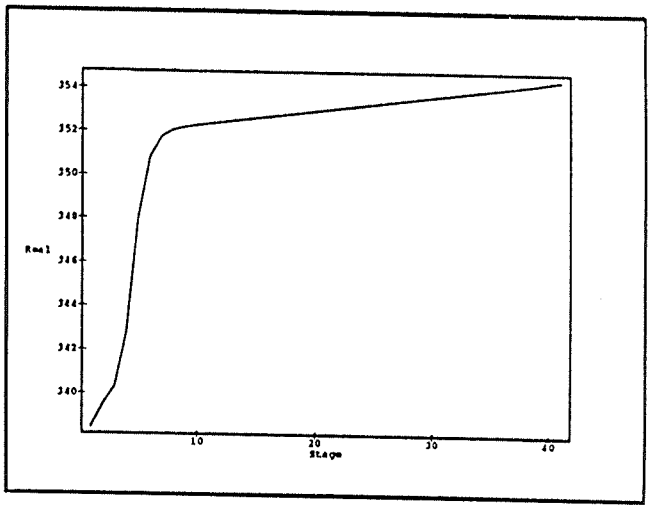

(d) Temperature Profile

Figure 3.18 Low Purity Real Solutions

Ethanol(1)-Benzene(2)-Water(3)

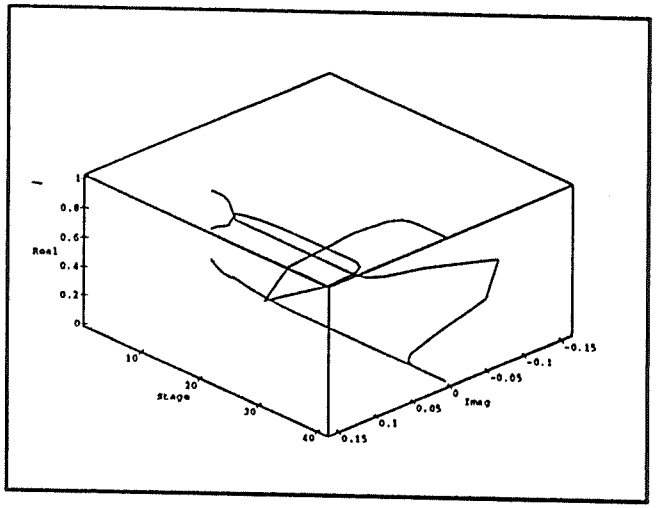

(a) 3 D View

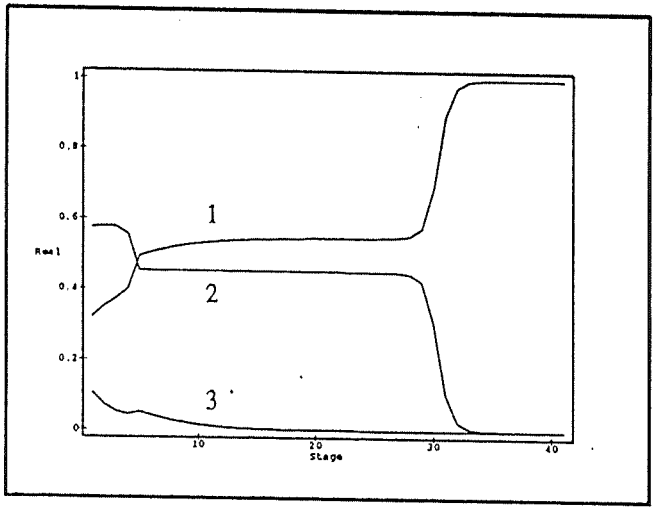

(b) Real Projection

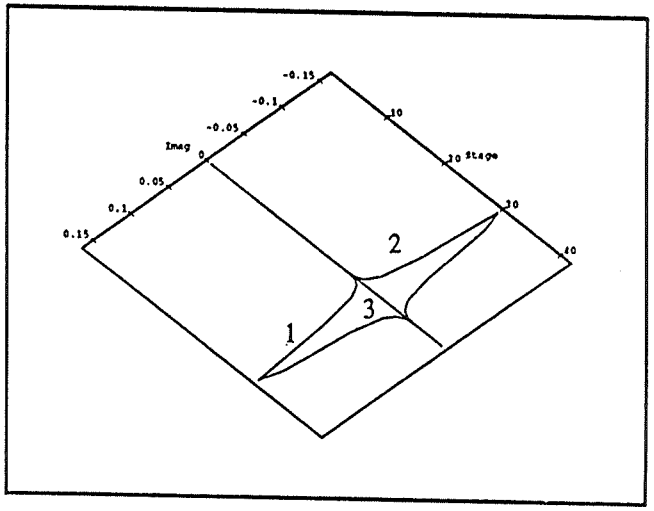

(c) Complex Projection

Figure 3.19 Complex High Purity Liquid Profiles

Ethanol(1)-Benzene(2)-Water(3)

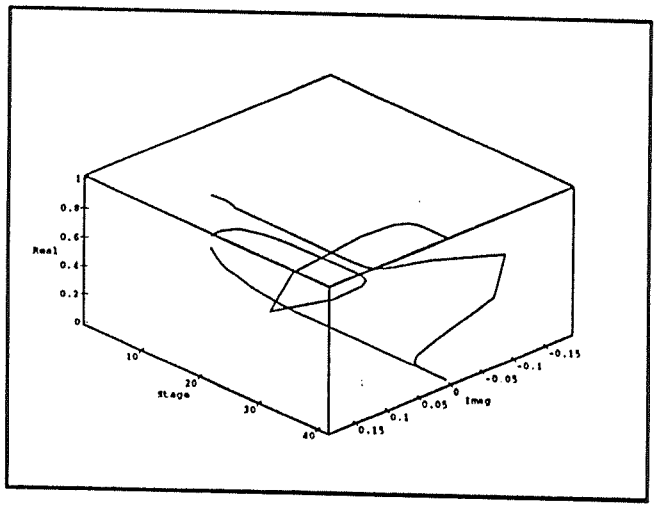

(a) 3 D View

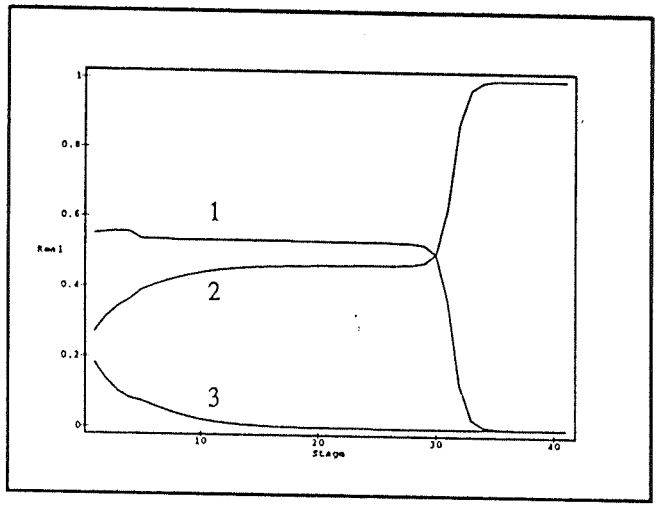

(b) Real Projection

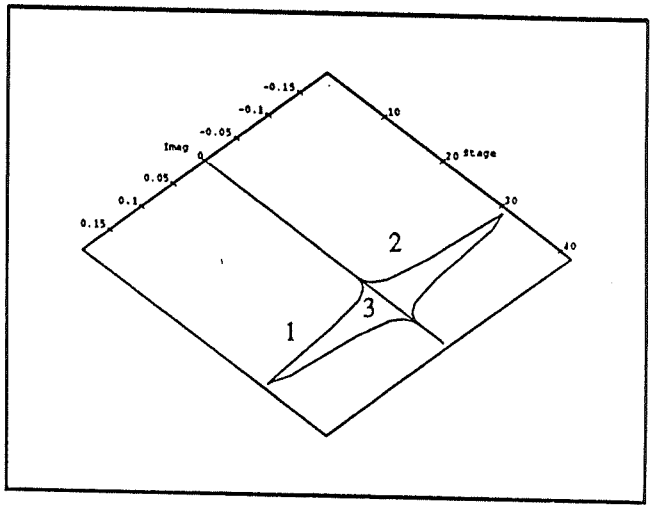

(c) Complex Projection

Figure 3.20 · Complex High Purity Vapor Profiles

Ethanol(1)-Benzene(2)-Water(3)

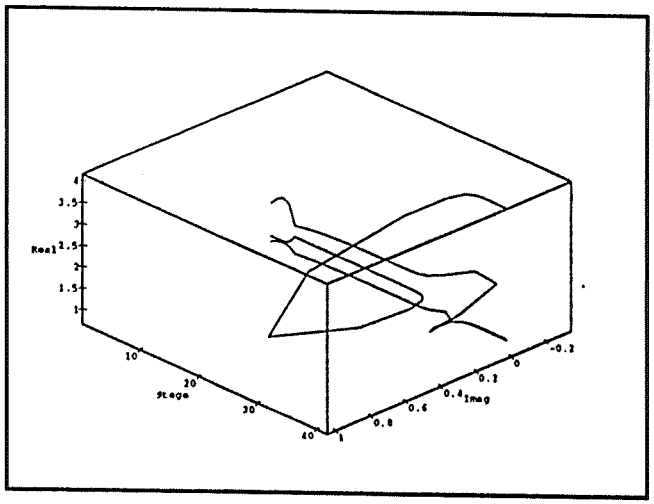

(a) 3 D View

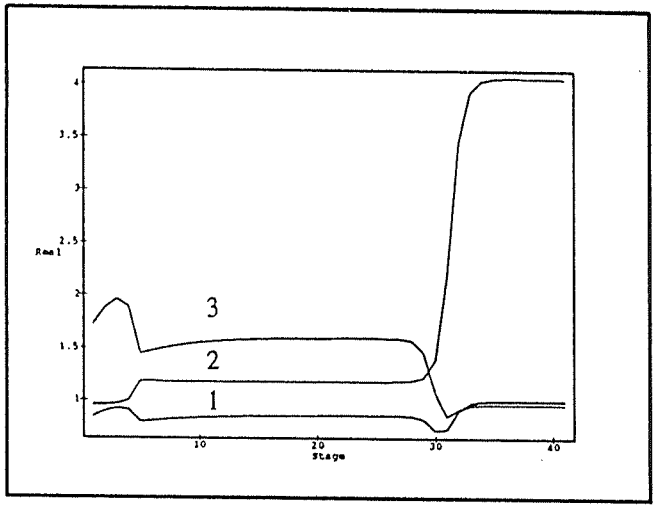

(b) Real Projection

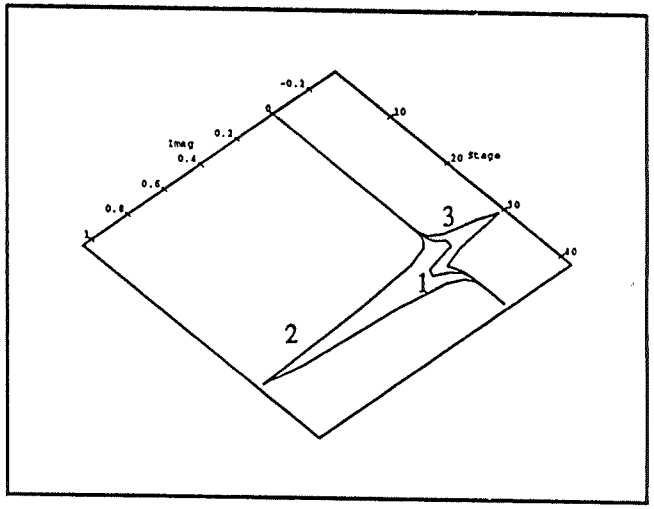

(c) Complex Projection

Figure 3.21 Complex High Purity K-Value Profiles

Ethanol(1)-Benzene(2)-Water(3)

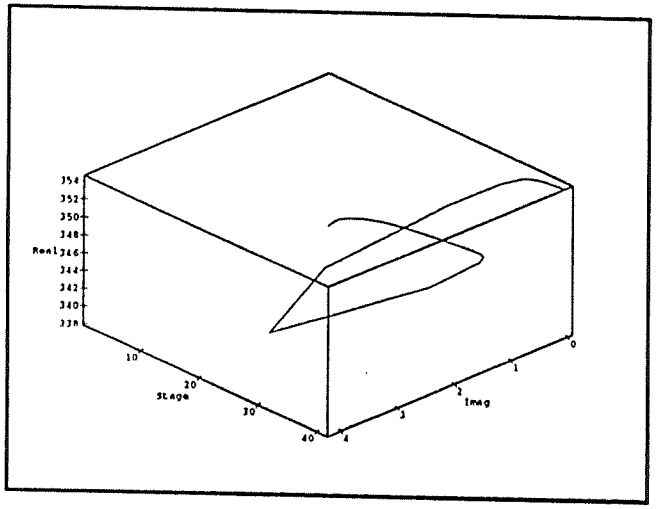

(a) 3 D View

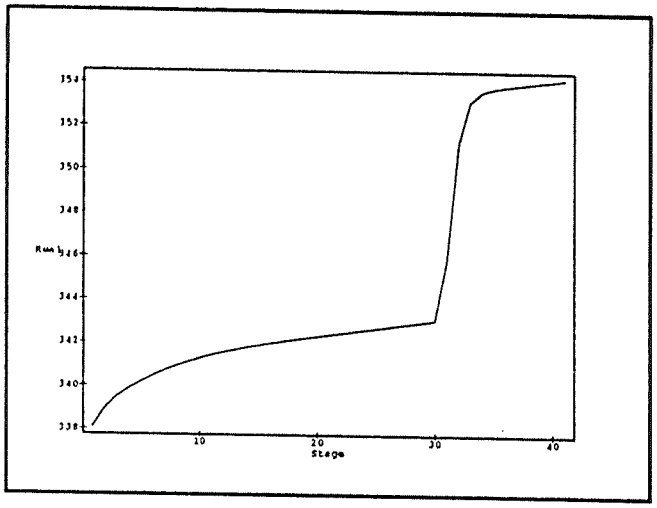

(b) Real Projection

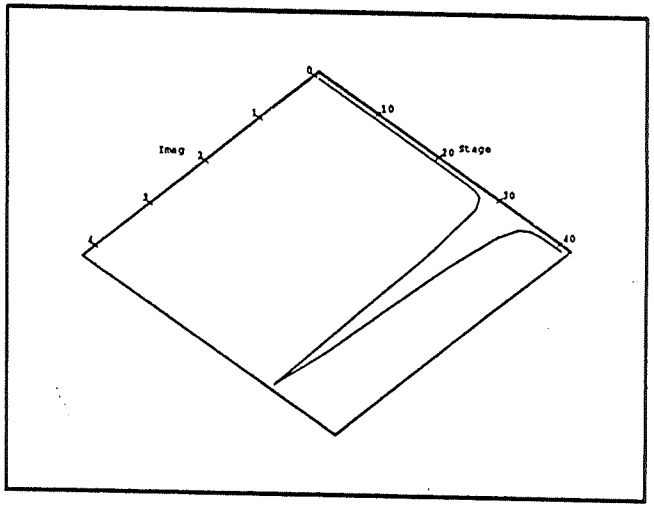

(c) Complex Projection

Figure 3.22 Complex High Purity Temperature Profile

Ethanol(1)-Benzene(2)-Water(3)

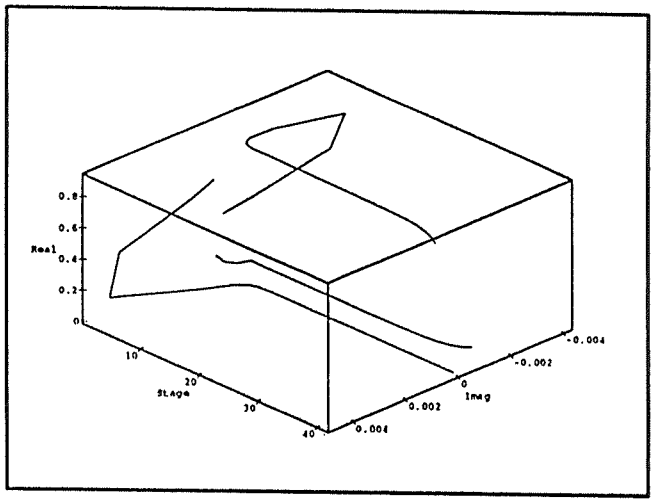

(a) 3 D View

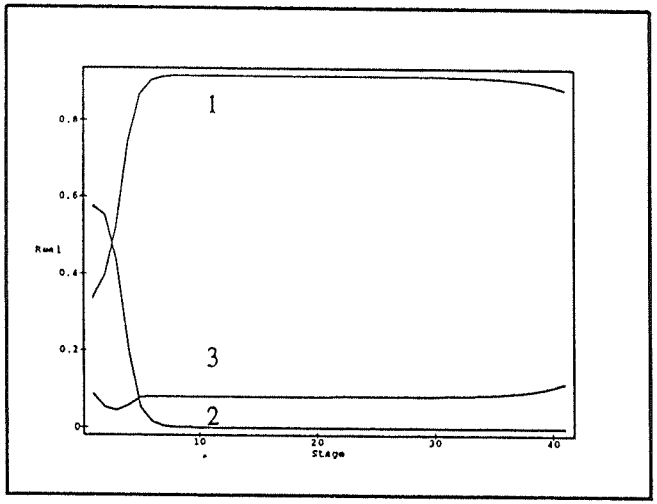

(b) Real Projection

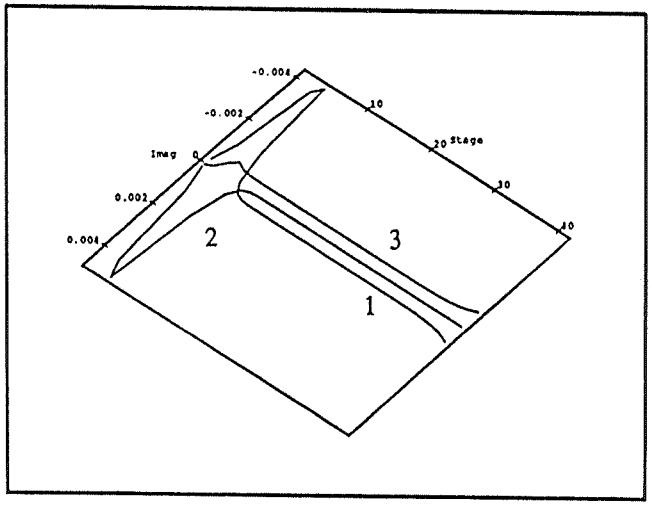

(c) Complex Projection

Figure 3.23 Complex Low Purity Liquid Compositions

Ethanol(1)-Benzene(2)-Water(3)

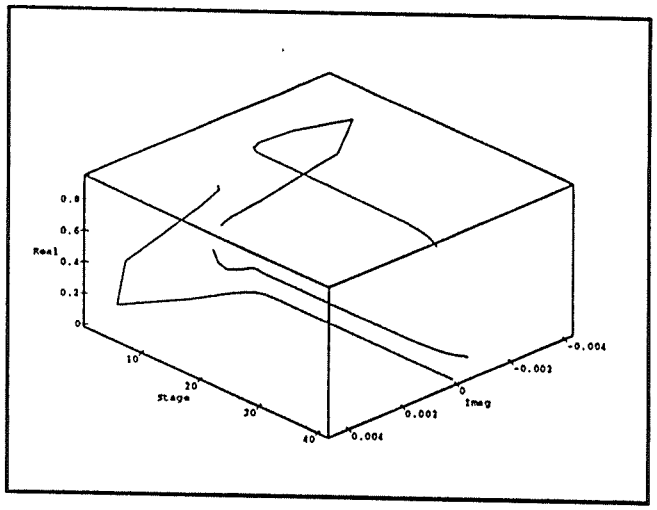

(a) 3 D View

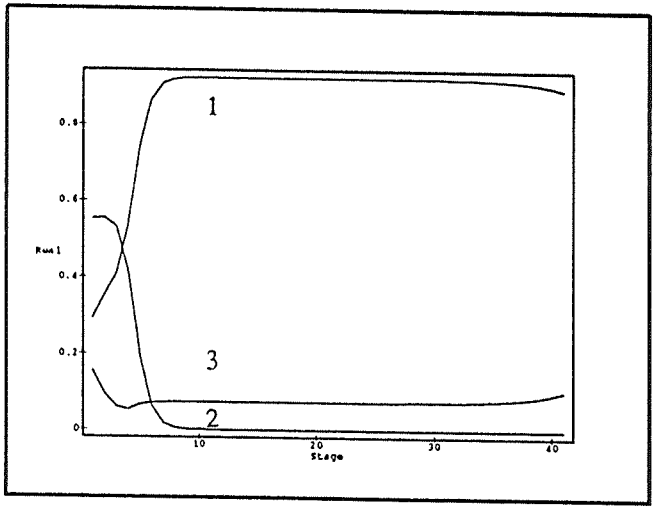

(b) Real Projection

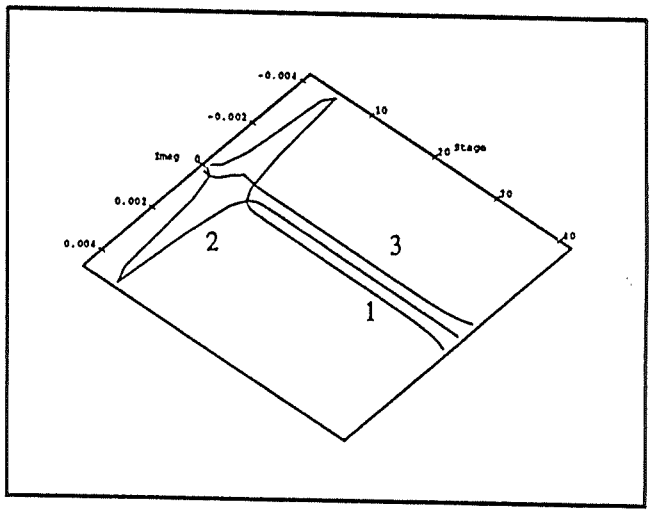

(c) Complex Projection

Figure 3.24 Complex Low Purity Vapor Compositions

Ethanol(1)-Benzene(2)-Water(3)

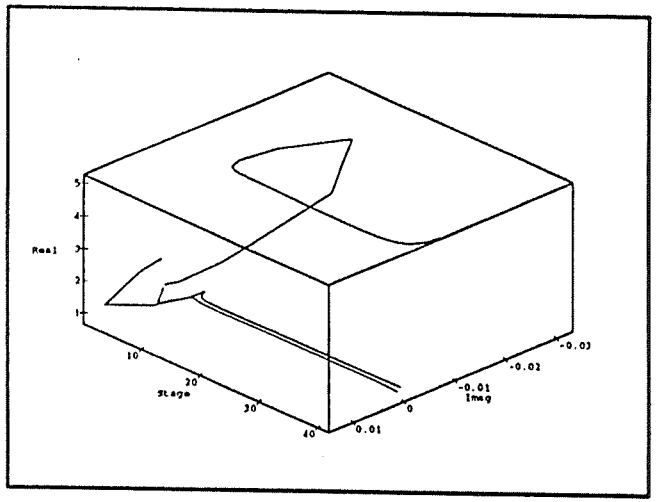

(a) 3 D View

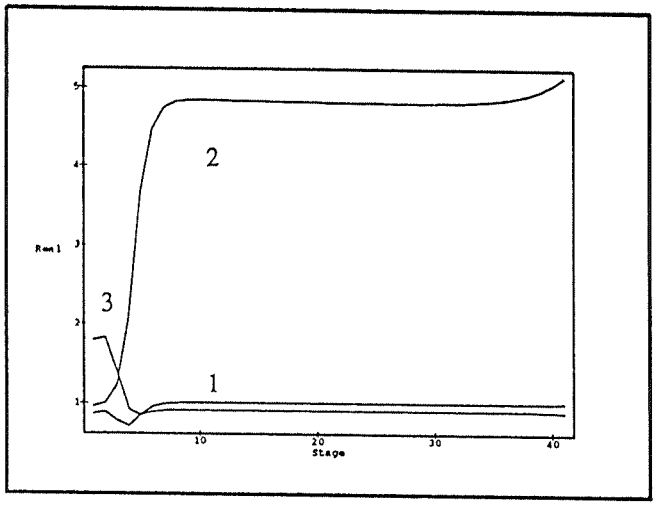

(b) Real Projection

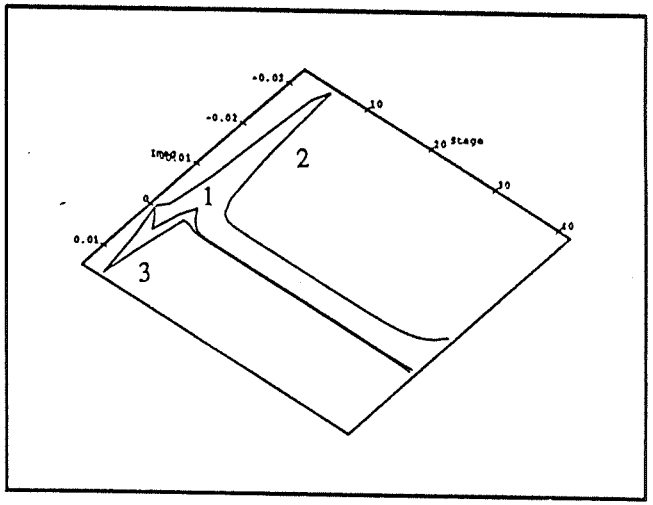

(c) Complex Projection

Figure 3.25 · Complex Low Purity K-Value Profiles

Ethanol(1)-Benzene(2)-Water(3)

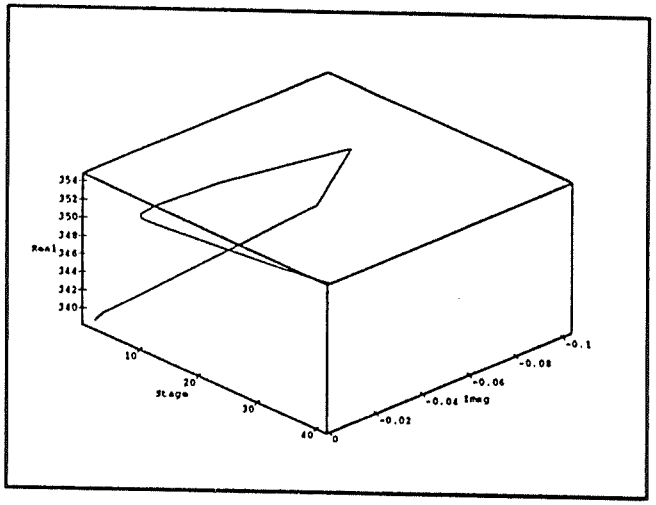

(a) 3 D View

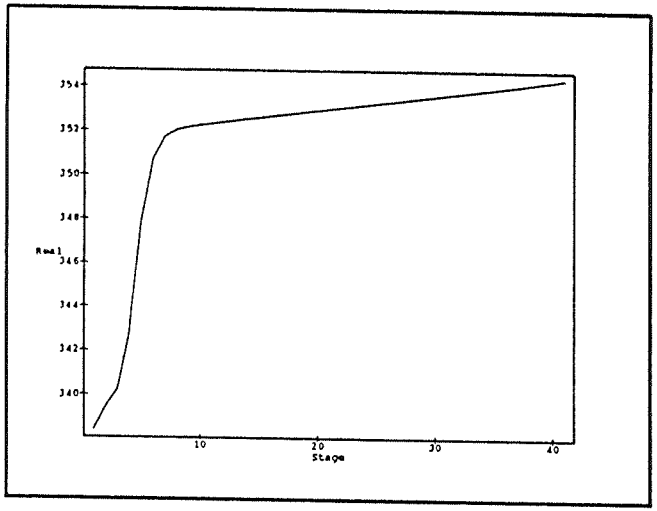

(b) Real Projection

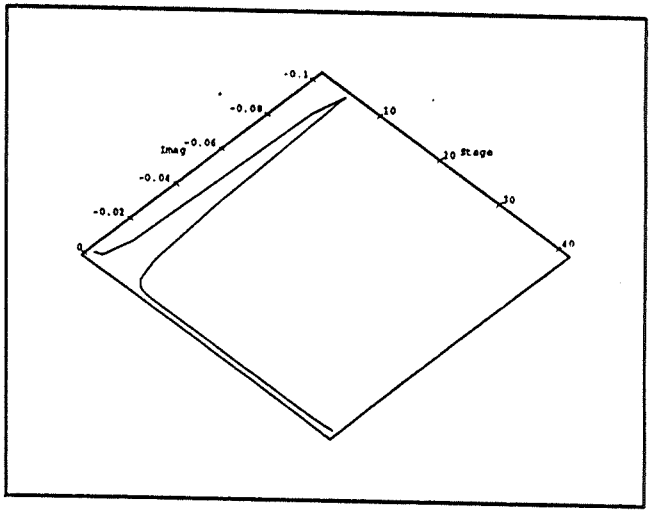

(c) Complex Projection

Figure 3.26 Complex Low Purity Temperature Profile

Ethanol(1)-Benzene(2)-Water(3)

3.4.5 The Acetone - Chloroform - Methanol System

Another system also exhibiting multiplicities that is considered is the acetone-chloroform-methanol system (Bekiaris et al., 1992). The azeotropic column operates at atmospheric pressure with constant pressure and has a total condenser is. The feed is introduced at the seventeenth stage. A schematic diagram of the column is shown in Fig. 3.27. Constant molar overflow and a tray efficiency of one are assumed. The vapor phase is considered ideal and the Wilson model is used to represent the liquid phase to ensure that any multiplicity is not due to the inappropriate neglect of potential liquid phase splitting.

The mole fraction of methanol in the bottoms product is shown as a function of reflux ratio in Fig. 3.28. The range of the reflux ratio varied from 1.5 to 80. Similar S-curves have been generated by Bekiaris et.al (1992) by plotting the acetone composition in the distillate against the distillate flow.

Real solutions of high and low purity near the turning points are shown in Figs. 3.29(a)-(d) and 3.30(a)-(d) respectively. Complex solutions were found near both of the turning points. The three dimensional views of the vapor and liquid composition, temperature and K-value profiles and their projections on to the real and complex planes for the high and low purity solutions are illustrated in Figs. 3.31(a) to 3.34(c) and 3.35(a) to 3.38(c) respectively. It is interesting to see the projections of these complex solutions on the real plane retain the same character even on bifurcation into the complex domain.

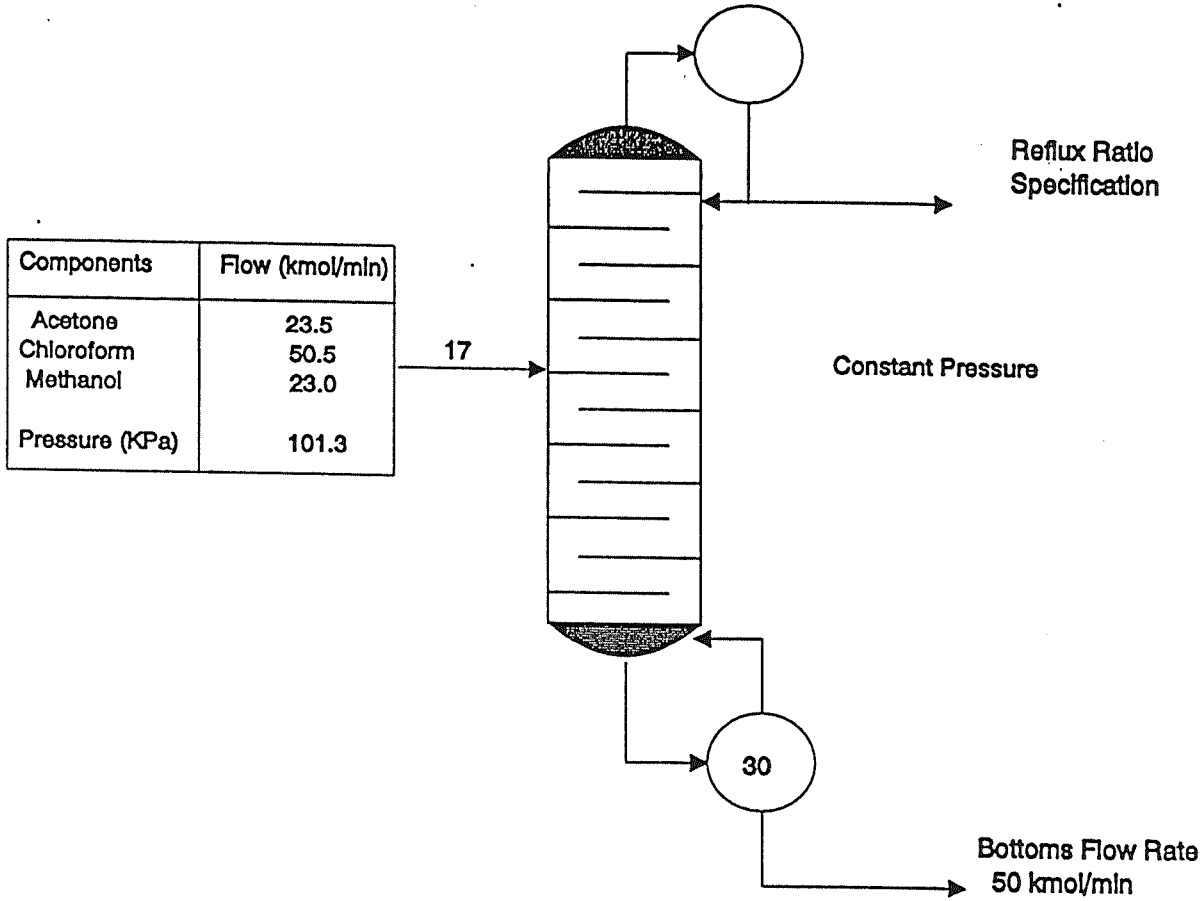

Figure 3.27 Azeotropic Distillation of Acetone-Chloroform-Methanol

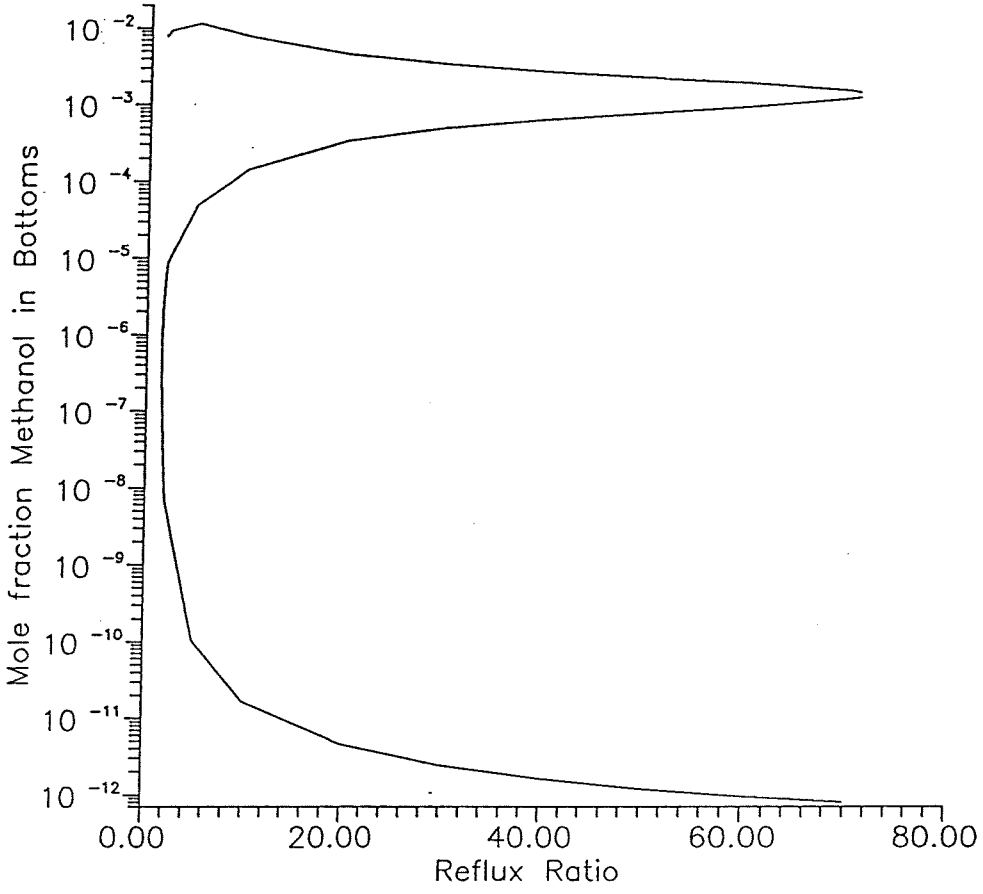

Figure 3.16 Bifurcation Diagram of Acetone–Chloroform–Methanol System

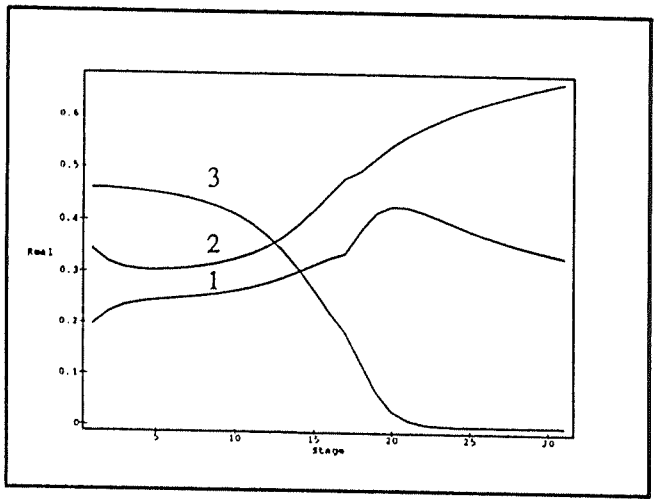

(a) Liquid Compositions

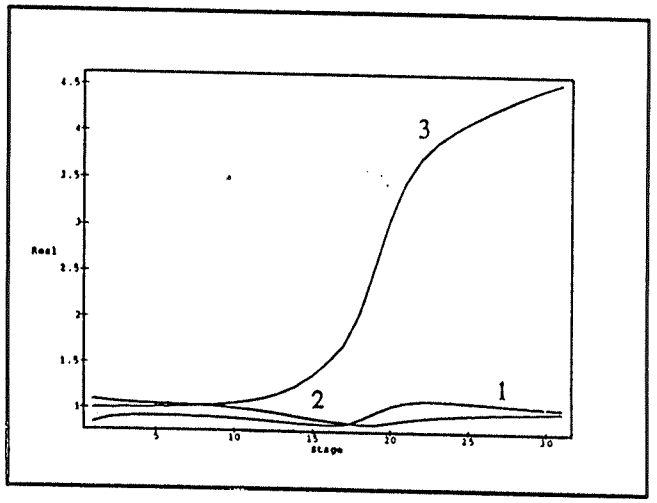

(b) K-Values

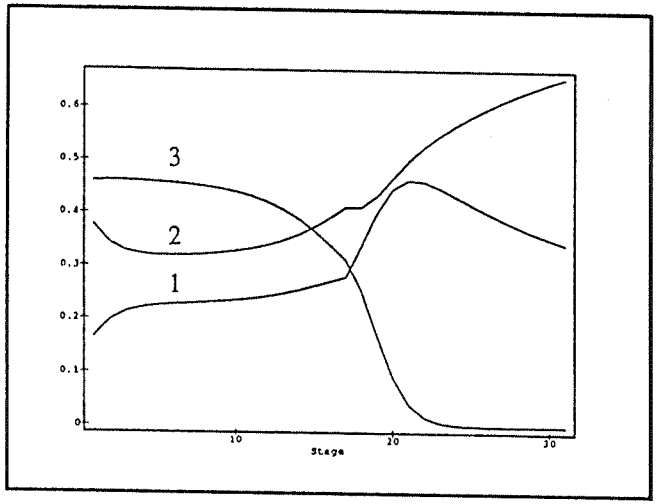

(c) Vapor Compositions

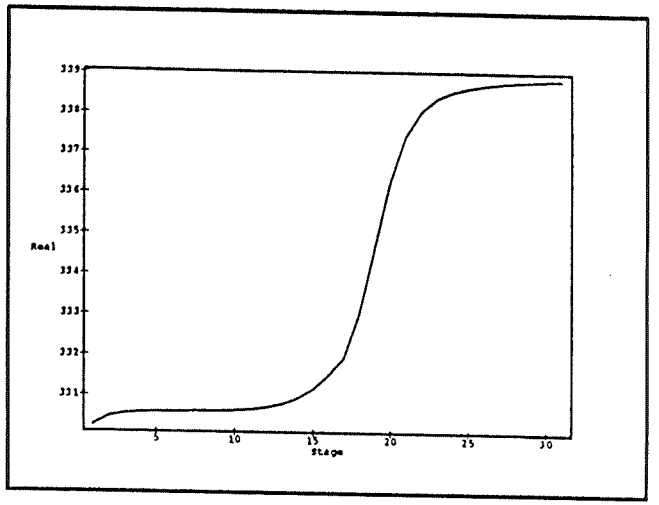

(d) Temperature Profile

Figure 3.29 High Purity Real Solutions

Acetone(1)-Chloroform(2)-Methanol(3)

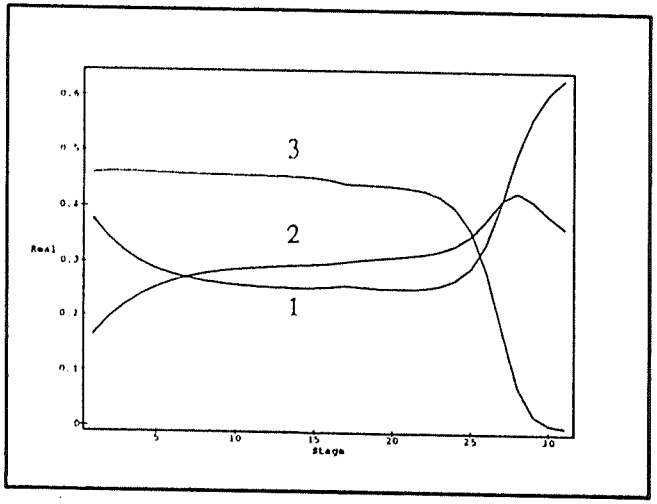

(a) Liquid Compositions

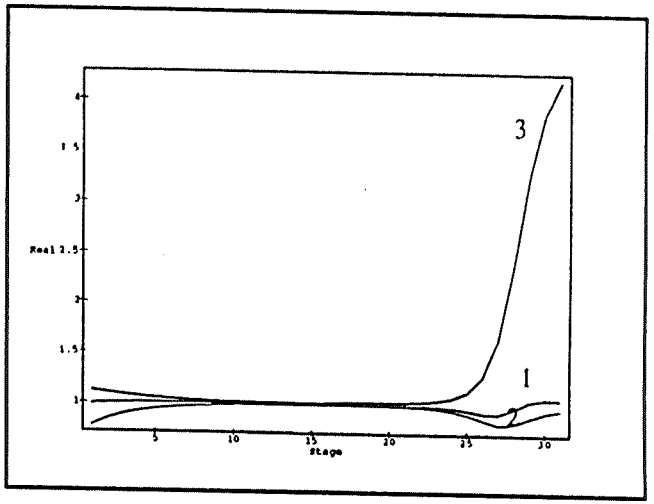

(b) K-Values

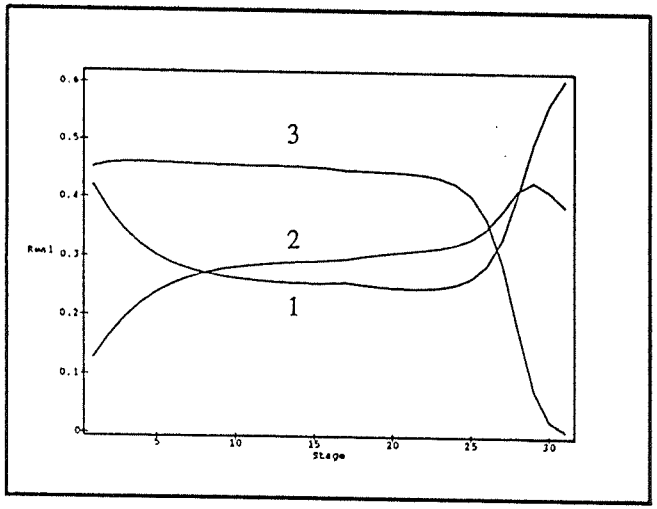

(c) Vapor Compositions

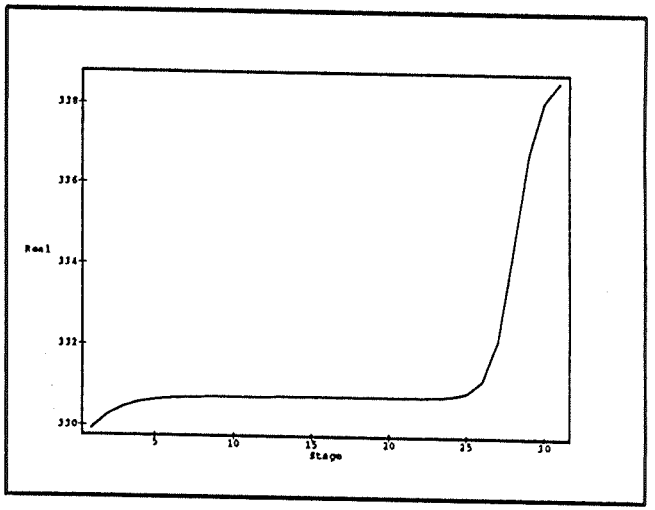

(d) Temperature Profile

Figure 3.30 · Low Purity Real Solutions

Acetone(1)-Chloroform(2)-Methanol(3)

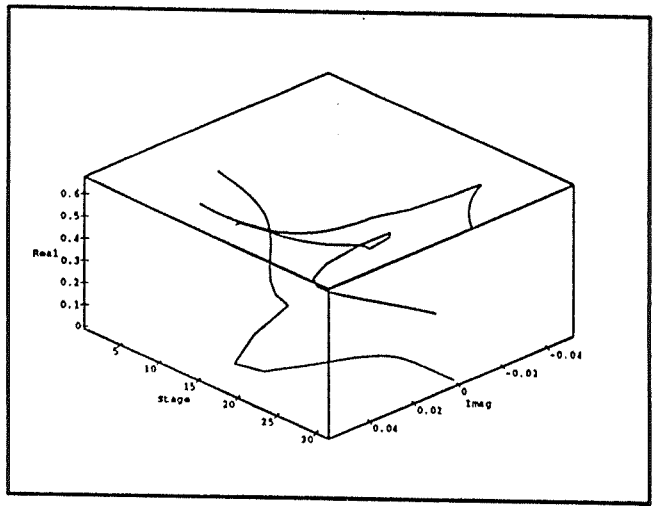

(a) 3 D View

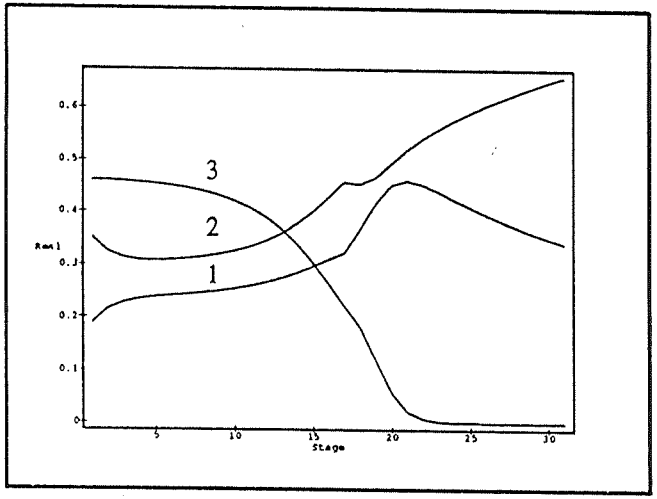

(b) Real Projection

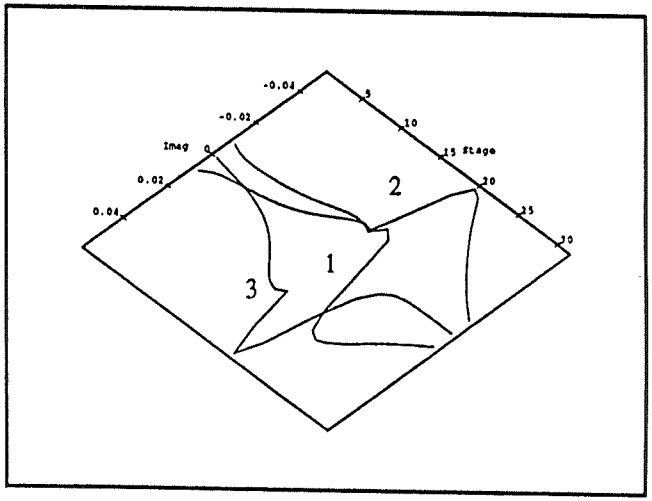

(c) Complex Projection

Figure 3.31 Complex High Purity Liquid Profiles

Acetone(1)-Chloroform(2)-Methanol(3)

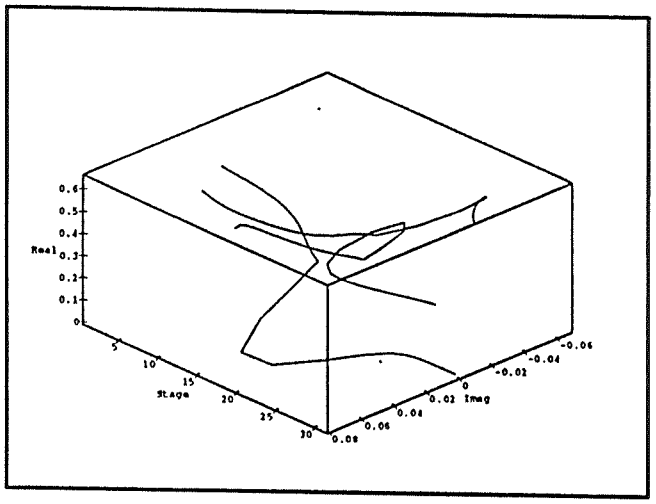

(a) 3 D View

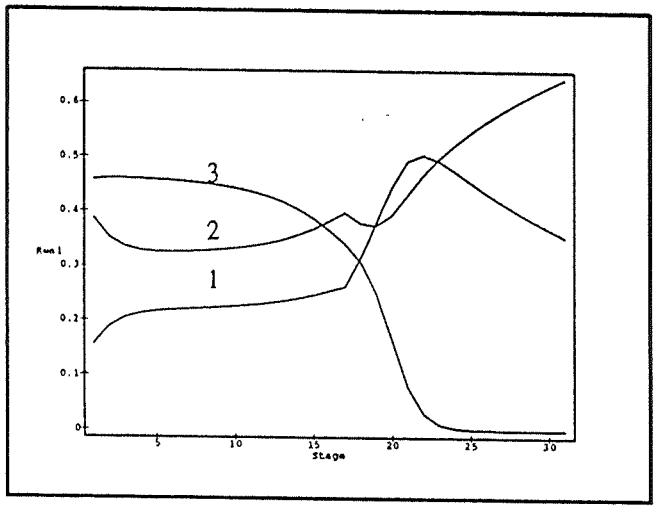

(b) Real Projection

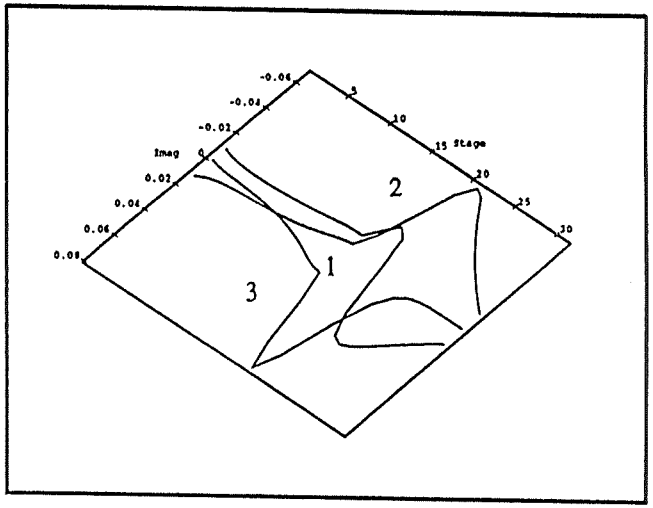

(c) Complex Projection

Figure 3.32 Complex High Purity Vapor Profiles

Acetone(1)-Chloroform(2)-Methanol(3)

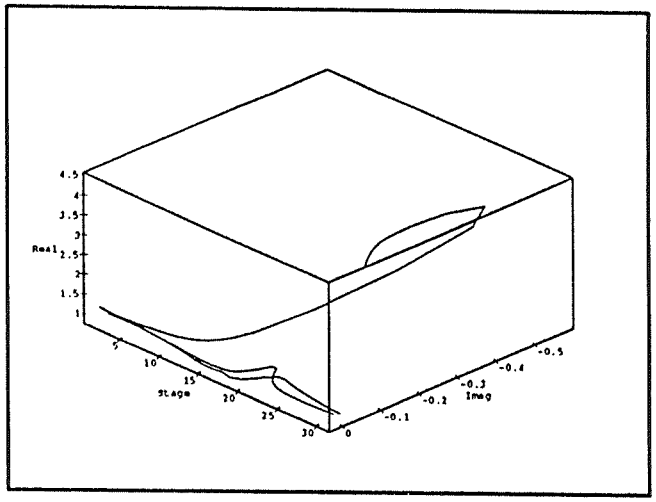

(a) 3 D View

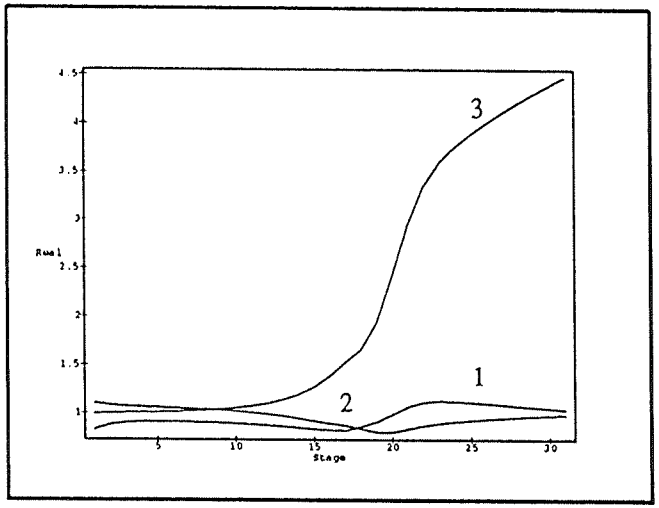

(b) Real Projection

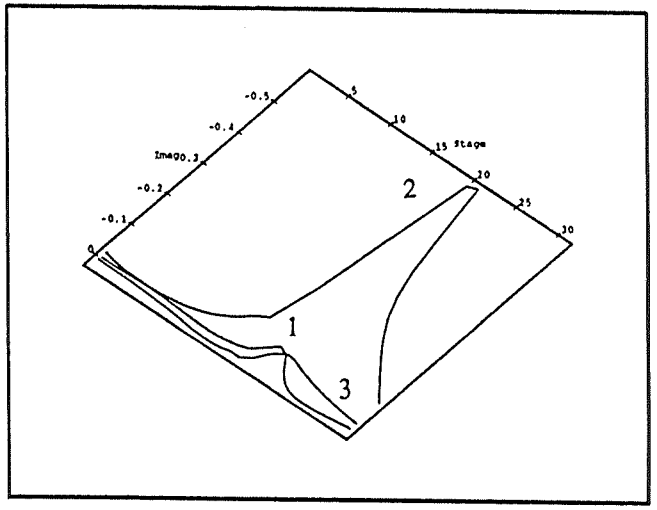

(c) Complex Projection

Figure 3.33 Complex High Purity K-Value Profiles

Acetone(1)-Chloroform(2)-Methanol(3)

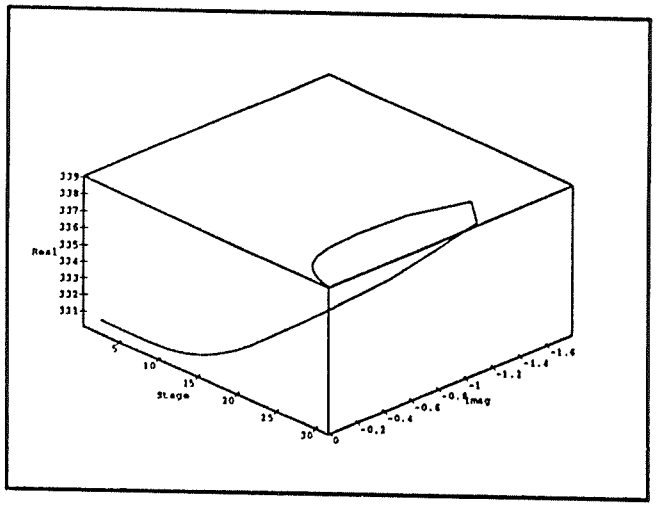

(a) 3 D View

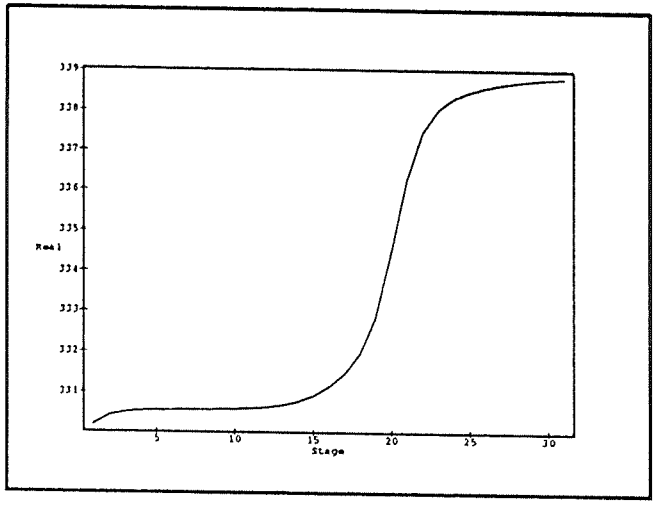

(b) Real Projection

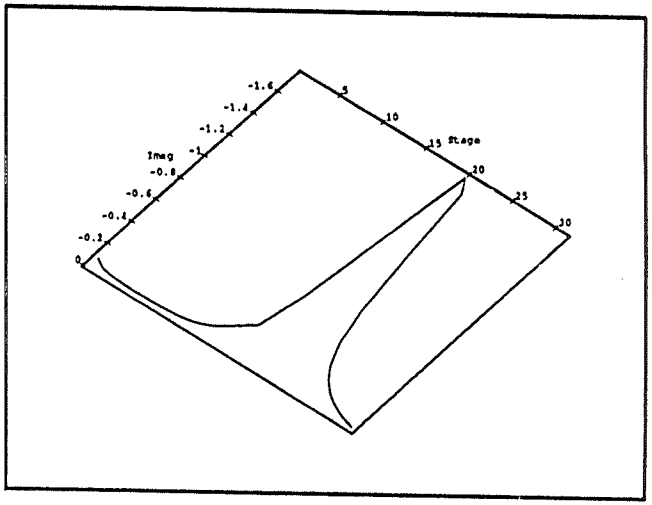

(c) Complex Projection

Figure 3.34 Complex High Purity Temperature Profile

Acetone(1)-Chloroform(2)-Methanol(3)

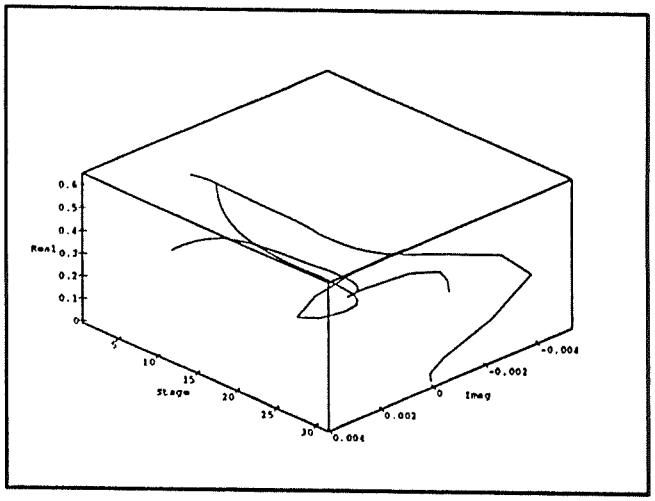

(a) 3 D View

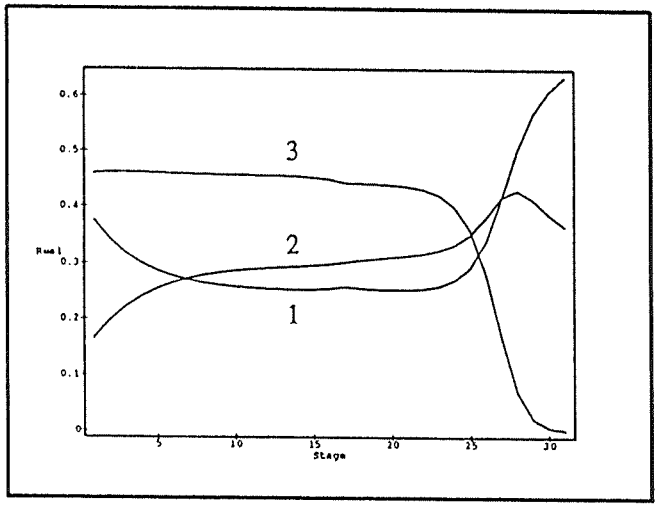

(b) Real Projection

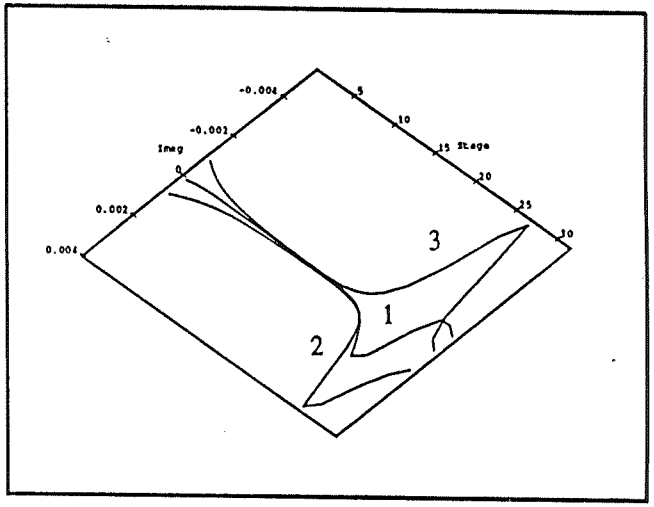

(c) Complex Projection

Figure 3.35 Complex Low Purity Liquid Profiles

Acetone(1)-Chloroform(2)-Methanol(3)

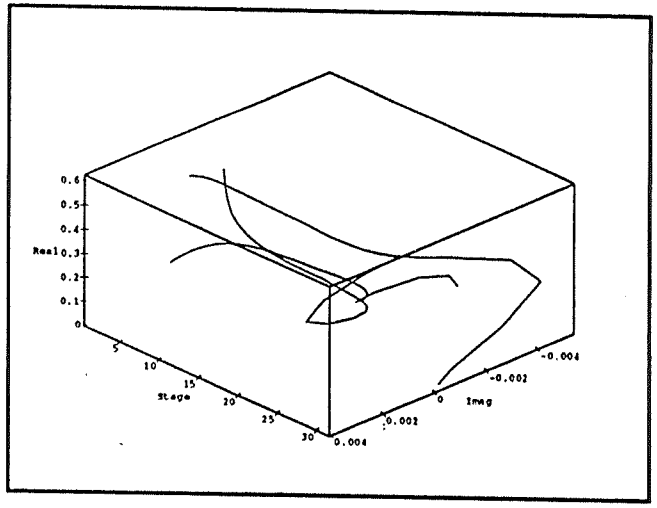

(a) 3 D View

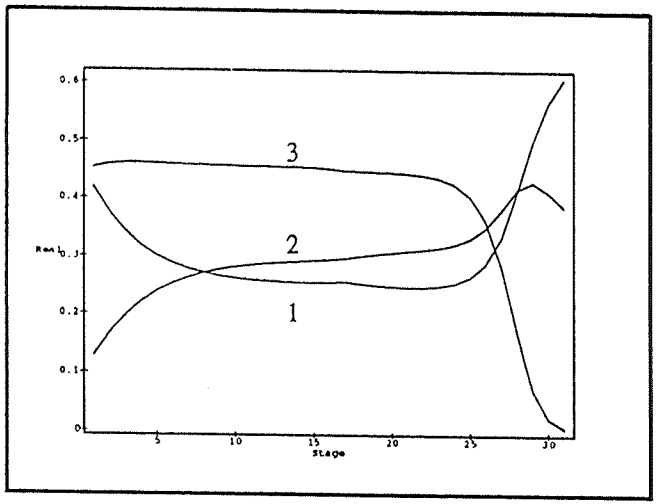

(b) Real Projection

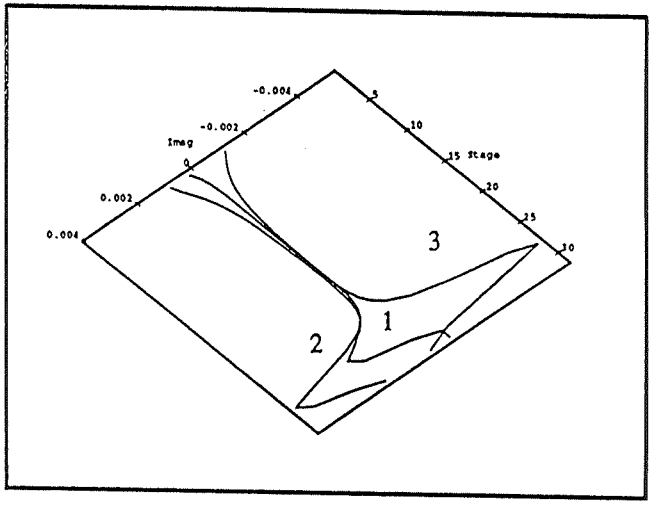

(c) Complex Projection

Figure 3.36 Complex Low Purity Vapor Profiles

Acetone(1)-Chloroform(2)-Methanol(3)

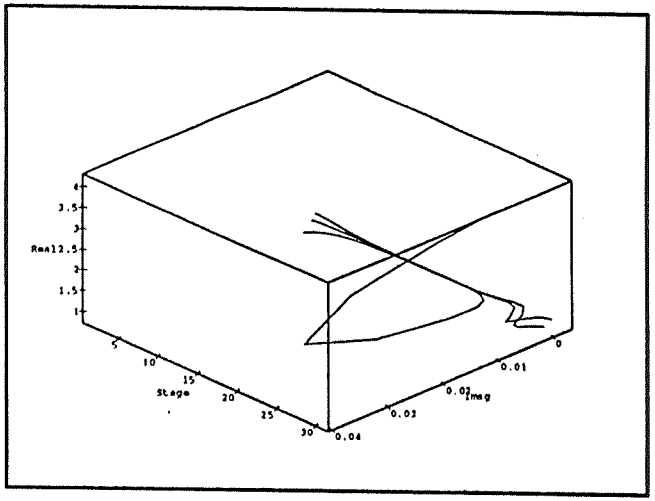

(a) 3 D View

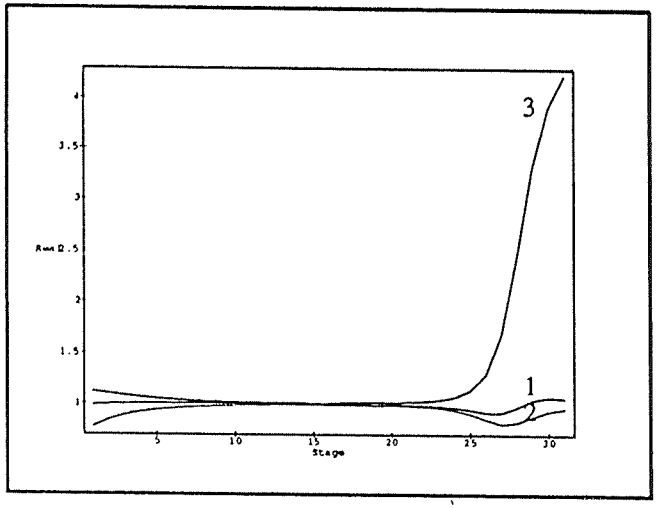

(b) Real Projection

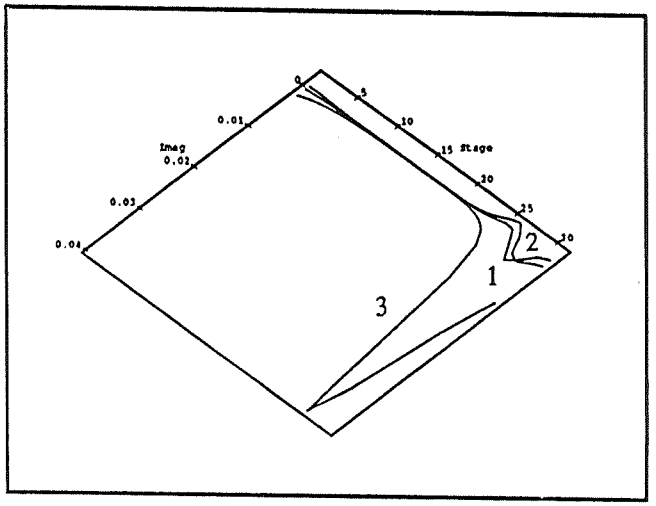

(c) Complex Projection

Figure 3.37 Complex Low Purity K-Value Profiles

Acetone(1)-Chloroform(2)-Methanol(3)

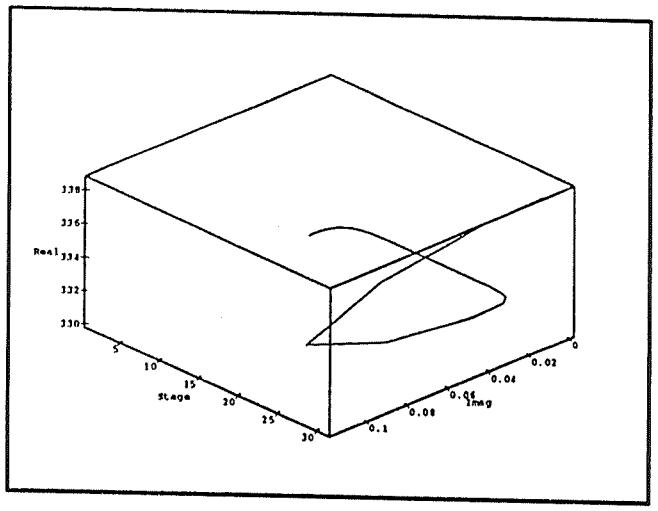

(a) 3 D View

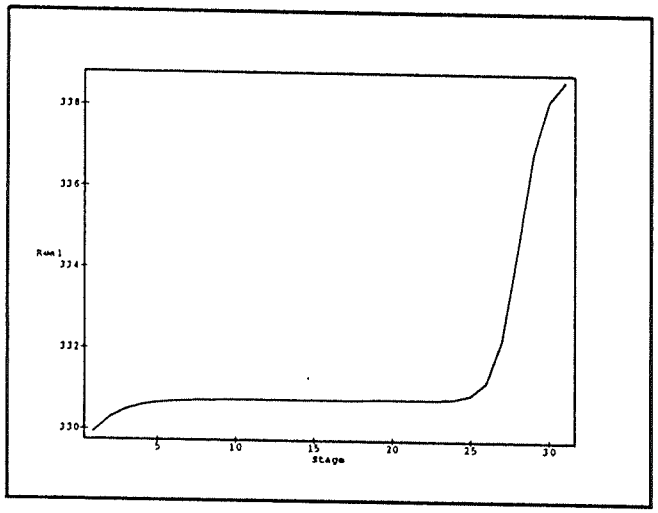

(b) Real Projection

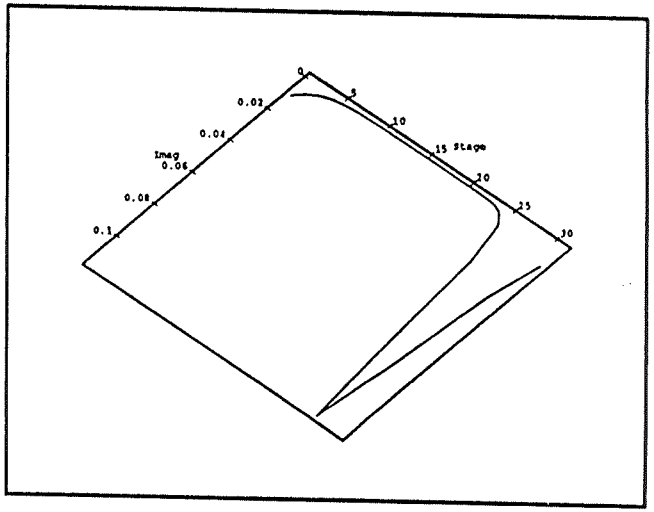

(c) Complex Projection

Figure 3.38 Complex Low Purity Temperature Profile

Acetone(1)-Chloroform(2)-Methanol(3)

3.5 COMPUTER TIME

A comparative study of the relative times taken by calculations in the real and complex domains was also made. The results are given in Table 3.5. This table shows the time taken to solve several representative problems. These represent actual industrial problems (two distillation plus one gas absorption and a liquid-liquid extraction) and they differ in their components, the models used for the thermodynamic property calculations, and the conditions of separation. It must be pointed out that these examples were chosen so that the number of iterations taken to solve each case, the iteration history and the converged solutions is the same in both the real and the complex domains. It can be seen that the complex domain calculations take up to three times longer than do the real domain calculations.

Table 3.5 Time Comparisons for Real and Complex Codes

Components/ Feed Flow (mol / s)	Total Stages/ Feed Stages	Model Used	Specifications	Real		Complex	
				Iter	Time (sec)	Iter	Time (sec)
Ethane/100 Propane/300 n-Butane/500 n-Pentane/100	20/10	PR EOS	Feed Pr. = 15atm Feed Temp =298K Reflux Ratio = 2.5 Bottom Flow rate= 600 mol / s	5	36	5	92
Methane / 0.0,20.2 Ethane / 0.0,46.6 Propane / 0.0,30.2 n-Butane / 0.0063,3.15 n-Pentane / 0.983,0.63 n-Nonane / 20.69,0.0	6 / 1,6	PR EOS	Feed Pr. = 27.58 Bar Feed Temp (K) = 305.4 K, 313.7 K No condenser No reboiler	6	30	6	56
n-Pentane / 50.0,0.0 Benzene / 50.0,0.0 Sulfolane / 0.0,100.0	10 / 1,10	UNIQUAC	Extractor Temp = 323.15 K	7	23	7	35
Benzene /10.9 Toluene /12.5 P-Xylene/7.8	30 / 16 Side streams 8,8	PR EOS	Reflux Ratio = 3.0 Bottom Flow rate= 20.23 mol / s	5	35	5	93

4 CONCLUSION

The objective of this study was to investigate the potential for performing multicomponent multistage separation process calculations. Some of the conclusions from the study include:

- It has been our observation that the complex code can solve certain problems far more easily than the real code. Specific examples include both flash and distillation problems. TP and PQ flash examples indicated that the complex code is capable of simulating mixtures near the critical regions and obtaining a nontrivial two phase solution. An industrial reboiled absorber problem could be solved in the real domain only for certain values of the bottoms specification while the complex code converged without any difficulty over a wide range of specifications. Similar results were obtained for the demethanizer of the Liquified Natural Gas plant. In both of these examples the mixtures were near their critical regions.

- For cases where a nontrivial solution was obtained by working in the real domain, repeating the calculations in the complex domain did not change the solution and a converged solution was obtained in the latter case in the same number of iterations.

- A time comparison between the real and the complex domain calculations indicated that complex calculations take up to about three times longer than do the real domain calculations. However, this is only a part of the whole picture. We have already shown that the complex code converges far more easily than the real code for same systems at high pressures in which the thermodynamic properties are calculated from an equation of state. In view of the fact that complex calculations can take significantly longer time due to the more cumbersome calculations involved, we would recommend that the calculations be performed in the real domain first and, in the event of failure (after a fairly limited number of iterations) be repeated in the complex domain.

- Complex solutions have been found for systems known to exhibit multiple real solutions. In all cases the complex solutions can be traced to a turning point in the S-curve that is a characteristic of systems exhibiting multiple solutions. Complex solutions have been obtained for a variety of activity coefficient models including the Wilson model. The presence of complex solutions may explain the reasons of the aperiodic or chaotic behavior near the bifurcation points in the real domain hence locating them are significant.

- No real or complex solution was obtained for problems that had been

provided with infeasible specifications especially when real purity specifications were made.

- Though working in the complex domain might help for certain problems, the iteration history in the complex domain can be as chaotic as in case the real domain.

- We have not been able to find complex solutions for systems whose thermodynamics are derived from the cubic equations of state. Complex solutions have been found by Lucia and Wang, 1993 for a VT flash problem with real temperature and feed specifications. Further, Lucia and Sridhar (1993) have shown that TP flashes involving cubic equations of state must have real-valued solutions.

REFERENCES

[1] Bekiaris, N., G. A. Meski, C. M. Radu, and M. Morari, "Multiple Steady State in Homogeneous Azeotropic Distillation", Ind. Eng. Chem. Res., 32 (9), 2023-2038 (1993).

[2] Christiansen, L. J., M. L. Michelson and A. Fredenslund, "Naphtali-Sandholm Distillation Calculaitons for NGL mixtures near the Critical Region", Comp. Chem. Eng., 3, 535-542 (1979).

[3] Gosset, R., G. Heyen, and B. Kalitventzeff, "An Efficient Algorithm to Solve Cubic Equations of State", Fluid Phase Equilibria, 25, 51-64 (1986).

[4] Gundersen, T., "Numerical Aspects of the Implementation of Cubic Equations of State in Flash Calculation Routines", Comp. Chem. Eng., 6 (3), 245-255 (1982).

[5] Kienle, A. and W. Marquardt, "Bifurcation Analysis and Steady State Multiplicity of Multicomponent, Non-equilibrium Distillation Processes", Chem. Eng. Sci., 46 (7), 1757-1769 (1991).

[6] Kooijman, H.A. and R. Taylor, "ChemSep, Yet Another Software Package for the Computer Simulation of Multicomponent Separation Processes", CACHE News, Fall 1992.

[7] Lawal, A.S., " A Consistent Rule for Selecting Roots in Cubic Equation of State", Ind. Eng. Chem. Research, 26, 857-859 (1987).

[8] Lucia, A. and R. Taylor, "Complex Iterative Solutions to Process Model Equations?",European Symp. Comp. Aided Process Eng., S387-S394 (1992).

[9] Lucia, A., X. Guo, P. J. Richey and R. Derebail, "Simple Process Equations, Fixed-Point Methods, and Chaos", AIChE J., 36 (5), 641-654 (1990).

[10] Lucia, A., X. Guo, and X. Wang, "Process Simulation in the Complex Domain", AIChE J., 39 (3), 461-470 (1993).

[11] Lucia, A., X. Wang, "Process Dynamics in Complex Domain",

Presentation at AIChE meeting, St. Louis, 1993.

[12] Lucia, A., J. Xu, "Global Minima in Root Finding", Recent Advances in Global Optimization, C. A. Floudas and P. Pardalos, Princeton University Press, Princeton, NJ (1992).

[13] Magnussen, T., M. L. Michelsen, and A. Fredenslund, "Azeotropic Distillation using UNIFAC', Inst. Che. Eng. Symp. Ser., 56, 4.2/1-4.2/19 (1979).

[14] Ohanomah, M.O. and D. W. Thompson, "Computation of Multicomponent Phase Eqauilibria-Part I. Vapor-Liquid Equilibria", Comp. Chem. Eng., 8 (3/4), 147-156 (1984).

[15] Perry's Chem. Eng. Handbook, 6th Ed., (1984).

[16] Reid, R. C., J. M. Prausnitz, and B. Poling, "The Properties of Gases and Liquids", 4th Ed., McGraw-Hill Publishers, 1987.

[17] Prokopakis, G.J. and W. D. Seider, "Feasible Specifications in Azeotropic Distillation", AIChE J., 29 (1), 49-60 (1983).

[18] Robinson, C. S. and E. R. Gilliland, "Elements of Fractional Distillation", McGraw Hill, (1950).

[19] Rovaglio, M. and M. F. Doherty, "Dynamics of Heterogeneous Azeotropic Distillation Columns", AIChE J., 36 (1), 1990.

[20] Sridhar, L. N. and A. Lucia, "Some Process Analysis in the Complex Domain", (Paper under Review).

[21] Taylor, R. and H. A. Kooijman, "Composition Derivatives of Activity Coefficient Models (for the estimation of thermodynamic factors in diffusion)", Chem. Eng. Commnn., 102, 87-106 (1991).

[22] Veerana, D. and D. N. Rihani, "Avoiding Convergence Problems in VLE Predictions using an Equation of State", Fluid Phase Equilibria, 16, 41-55 (1984).

[23] Veerana, D., A. Husain, S. Subramaniyam and M. K. Sarkar, "An Algorithm for Flash Calculations using an Equation of State", 11 (5), 489-496 (1987).

[24] Venkataraman, S. and A. Lucia, "Solving Distillation Problems by Newton-Like Methods", Comp. Che. Eng., 12 (1), 55-69 (1988).

[25] Walas, S.M., "Phase Equilibria in Chemical Engineering", Butterworth Publishers, 1985.

[26] Whitson, C. H. and M. L. Michelsen, "The Negative Flash",Fluid Phase Equilibria, 53, 51-71 (1989).

NOMENCLATURE

A_j	Elements of subdiagonal matrix at stage j in Eqn. 31
A	Equation of state parameter
B_j	Elements of diagonal matrix at stage j in Eqn. 31
B	Equation of state parameter
c	Number of components
C_j	Elements of superdiagonal matrix at stage j in Eqn. 31
e_j	Number of equations
E	Equilibrium relations given by equilibrium model
f	Fugacity coefficient in Eqn. 18
f	Vector of discrepancy functions defined by Eqn. 20
F	Feed flow rate
F	Functional representation of cubic equationof state defined by Eqn. 26
F	Rachford-Rice function defined by Eqn. 28
H	Heat balance equations in equilibrium model
[J]	Jacobian matrix defined by Eqn. 23
K_i	Equilibrium constants of component i
L	Liquid flow rate
M	Mass balance equations in equilibrium model
n	Number of stages
P	Pressure

Pr	Reduced pressure
Q_j	Heat duty in equilibrium stage model
R_j	Right hand side matrix elements in Eqn. 32
r_j	Ratio of sidestream flow to interstage flows
S	Summation equations given by equilibrium model
T_j	Temperature at stage j
U_j	Interstage liquid flow
V_j	Vapoe flow rate
W_j	Interstage vapor flow
x_i	Liquid compositions of component i
y_i	Vapor compositions of component i
z_i	Feed compositions of component i
Z	Compressibility root

SUBSCRIPTS

i	Component i
j	Stage j
k	Current iteration number

SUPERSCRIPTS

L	Liquid
V	Vapor

F Feed

GREEK SYMBOLS

γ_i Activity coefficient of component i

ϵ a small number

μ_i Chemical potential of component i

Φ_i Vapor fraction in Eqn. 28